The University of Manitoba

Department of Mechanical Engineering

Improving the Fatigue Strength of Loaded Holes by the Dimpling Process

A thesis by

Frank A. Roberts

Submitted in partial fulfilment
of the requirements
for the degree of

Master of Science in Mechanical Engineering

May 1973

Acknowledgments

Gratitude is extended to my advisor, Dr. John Shewchuk, for his invaluable guidance and assistance. Also to Dr. J. Cahoon and the Metallurgy Group of the Department of Mechanical Engineering for freely making available information and expertise.

Thanks are also due to the Department of Civil Engineering for the loan of equipment and to the National Research Council of Canada for their financial assistance.

Table of Contents

Table of Contents (continued)

List of Tables

List of Figures

List of Figures (continued)

List of Figures (continued)

Nomenclature

S_{oa}	alternating octahedral shear stress
S_{om}	mean octahedral shear stress
S_e	endurance stress for 10^6 cycles to failure
K_f	fatigue strength reduction factor
S_a	alternating normal stress
S_m	mean normal stress
S_y	yield stress
n	integer, order of reflection
λ	wave length of incident x-ray
d	material lattice parameter
θ	angle of incidence
ε_3	normal strain
ε_z	normal strain
l_z	gauge length
d_n	strained lattice parameter in the normal direction
d_o	unstrained lattice parameter
ϕ	azmuthal angle for the direction of strain measurement
ψ	angle of inclined incidence to surface normal
ε_ψ	strain in the ψ direction
d_ψ	strained lattice parameter in the ψ direction
σ_ϕ	stress in the ϕ direction
E	elastic modulus
υ	Poisson ratio
S	radius of the diffraction ring

Nomenclature (continued)

D	specimen to film distance
S_i	radius of the diffraction ring at inclined incidence
S_n	radius of the diffraction ring at normal incidence
ξ	$180^o - 2\theta$
K_t	theoretical stress concentration factor
F	load in pounds
σ	nominal stress on drilled specimen
σ_p	stress at the hole edge
d	die diemeter
i	indentor diameter
h	thickness of material

Chapter 1

Introduction

1.1 Introduction

The beginning of the twentieth century saw designers puzzling over brittle-type failures in presumably ductile materials occurring after a lengthy service life. These "fatigue" failures as we now know them continue to be one of the most perplexing problems which a mechanical designer must face.

The study of fatigue has been inspired both by industry and the general public. The catastrophic nature of fatigue failures has more than once captured the attention of the public as structures used repeatedly and supposedly safe, fail without warning. Demands for action have challenged many researchers to provide insights into the topic. With ever increasing requirements of speed, compactness and lengthy service, fractures resulting from fatigue now represent in excess of 90% of all service failures. From this figure it may be surmised that control of fatigue failures is of foremost concern to those industries affected. Many industries have found it necessary to conduct extensive fatigue research.

The first investigations on fatigue were directed towards material properties as early hypotheses suggested that fatigue caused changes in physical structure. The dynamic properties first of iron and steel, then

aluminums and eventually all metals have since been carefully examined and tabulated. Later studies led to increased understanding of the failure mechanisms, crack nucleation and crack propagation. Other efforts have been towards the accurate prediction of material life and strength using this accumulated knowledge. Research by scientists and engineers and a century of experience documented in journals around the world have produced data on almost every usable structural material. Even so, it can hardly be said that fatigue failures have ceased or in future ever will cease.

The cardinal point remains, that fatigue is a highly localized phenomenon and cracks may begin at any point where tensile stresses are high, regardless of the nominal stress level. In practice fatigue failures are almost invariably located in these areas of high stress - bolt or rivet holes, section reductions, welds or seams. The overall performance of any structure is determined not by its greatest strength but by its greatest weakness. Joints and connections of a structure are that weakness, and any serious attempts to improve the fatigue strength of components must give cognisance to this fact. Unfortunately this is one area where the designer is at a serious disadvantage. The reams of data available are ineffective in predicting the fatigue strength of even simple joints.

To design a joint with strength equal to that of the member the joint must either be of much larger section or the stress distribution must somehow be altered to reduce peak stresses. It is evident that where size and weight are crucial factors the former design philosophy is not practicable. In preference, a designer should select a local strengthening mechanism to spread loads more evenly across connected parts, achieving higher joint efficiency and correspondingly higher strength to weight and volume ratios.

Efforts by many researchers to improve the fatigue strength of connections are described in this thesis. A great deal is known about materials and fatigue failure mechanisms; it remains only to apply this knowledge is an intelligent manner to the more complicated case of joints.

1.2 Statement of Problem

This thesis proposes and studies the effectiveness of a new method for increasing the fatigue strength of loaded hole connections in sheet materials. This method, known as the "Dimpling Process" functions by inducing beneficial residual stresses at concentrations. The residual stresses are measured experimentally for use in predictions of fatigue strength improvement. Predictions are compared with actual fatigue data from processed and unprocessed specimens. This work examines several versions of the process and corresponding fatigue strengths.

1.3 Scope of Thesis

A new process for increasing the fatigue strength of loaded holes in sheet materials will be introduced and discussed in five chapters and related appendices.

Chapter 1 provides background on fatigue research on materials and components.

Chapter 2 is a review of previous research on fatigue strength improvement techniques for loaded holes.

Chapter 3 describes a new fatigue strength improvement process for loaded holes and predicts the extent of improvement based on measured residual stresses.

Chapter 4 describes fatigue testing on processed loaded-hole specimens, comparing results with predictions and tests on other processes.

Chapter 5 gives a summary and conclusions.

Appendix A describes the measurement of residual stresses in processed specimens.

Appendix B describes a method of residual stress determination using comparative brittle lacquer-tension tests.

Chapter 2

Progress in Fatigue Strength Improvement of Loaded Holes

2.1 Introduction

The design of loaded hole connections is basic to the more general topic of joint design. Loaded holes have been and continue to be a major source of fatigue failures everywhere that repeated loads are encountered. Researchers in this area have proposed and tested numerous techniques to improve fatigue strength and have met with varying degrees of success. The following literature survey is a summary of notable advances describing the processes and the relative effectiveness found by each experimentor.

2.2 Literature Review

The effects of clamping at a loaded hole were investigated by Mittenbergs and Beall (5) and Heywood (3). Clamping reduced shear stresses at the holes by transferring a part of the load through friction. Mittenbergs and Beall experimented with a single torque bolt connection under steady axial tension and fully reversed bending. Fatigue strength was found to increase proportionally with bolt torque up to a threshold torque of 300 ft.-lb. beyond which all load was transferred through friction. Further increases in torque produced diminishing strength improvements. With the change in mode of

load transmission it was found that failures moved from around the holes to the faying surfaces where fretting prevailed. For the optimum bolt torque of 300 ft.-lb. the allowable bending stress at 10^6 cycles was approximately doubled. Heywood investigated clamping effects on five bolt, double shear joints loaded in alternating tension. He concluded that:

"1) Clamped joints should be of ... short length. This in turn means that elastic straining actions of inner and outer members become relatively unimportant and hence there is usually no need to taper members.

2) Clamping makes the inner and outer members behave integrally as if welded together. This reduces stress concentrations at holes since both the distortions of members and bolt bending effect are reduced. In fact, the weakest point is usually away from the hole boundaries at some region of fretting ...

3) Since load is not transferred through the bolts, generous clearance holes and tolerances on bolt pitch are possible.

4) The joint efficiency is highest when the inner member is thin compared with its width, and lowest when the member is of square section."

The joint efficiency as used here was defined as the alternating load applied to the joint divided by the alternating load applied to a plain specimen of the

same section for the same number of cycles to failure. Since the load was transmitted entirely through friction, uniform pressure was necessary to reduce slipping and subsequent fretting. Use of a short joint as suggested in item 1 was beneficial. With 100% clamping the site of failure initiation became the faying surfaces as illustrated in Fig. 2.1. Heywood solved this by undercutting so that fretting occurred only in areas of low stress as illustrated in Fig. 2.2. One service problem was that to insure sufficient clamping, bolts had to be retightened occasionally. Heywood found remarkably high improvements. His results are presented in Table 2.1.

A number of researchers have examined the change in fatigue strength resulting with varying amounts of pin interference and pin clearance. Three simultaneous effects contribute to the strength improvement of interference fits. Firstly, the pin is rigidly fixed within the joined members. This results in reduced slippage and pin bending which correspondingly reduces fretting and high localized stresses. Secondly, the interference fit induces tensile stresses in the material surrounding the pin. By superposition this would increase the maximum stress at the pin, but as the external load is applied the tensile reaction stresses are relieved. The net effect is to somewhat increase the mean stress while substantially diminishing the alternating stress. The large decrease in alternating stress results

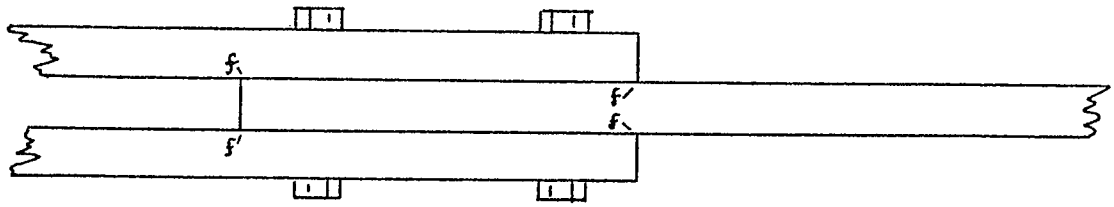

Figure 2.1. Double-shear clamped joint tested by Heywood (3) pp. 219-223. Regions of fretting (designated 'f') are highly stressed.

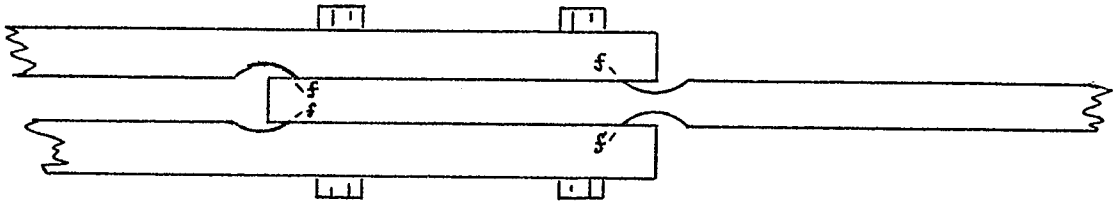

Figure 2.2. Double-shear clamped joint which has been undercut. Regions of fretting (designated 'f') are at low stress.

Table 2.1

Fatigue Life and Strength of Clamped vs. Aircraft Joint*

Base Life or Strength	Clamped Joint A	Typical Aircraft Joint B	Ratio A/B
Life at 19.8 $\pm$ 6.58 ksi	2,000,000	29,000	70
Alternating Stress for σ_m = 19.8 ksi N = 2 x 10^6	$\pm$ 6.58 ksi	$\pm$ 1.88 ksi	3.5

* Heywood (3)

in strength improvements far outweighing decreases resulting from increased mean stress. Finally, the interference fit causes a portion of the load to be transmitted by shear at the transverse diameter of the pin. The subsequent redistribution of load lowers the effective stress concentration.

Clearance fits function by decreasing contact along the edges, the area of greatest slippage and highest stresses. Fretting is thus eliminated in this area and moved to an area of lower stress and longer path of propagation.

White (10) studied both clearance and interference fits in double shear joints of FV 520B steel under pulsating tension and then constant mean stress with varied alternating tension. His results, shown in Fig. 2.3, indicate that both increasing clearance or interference produce improvements in fatigue strength.

Low (4) examined interference fits in a pinned lug of L65 aluminum alloy under axial tension. The results for this joint, which was fashioned after an actual aircraft joint, are presented in Fig. 2.4. It can be seen that considerable improvement was obtained with increasing interference, the optimum being .007 in. interference for a 1 in. pin. This produced a threefold increase in fatigue strength at 10^6 cycles and an eightfold increase at 10^7 cycles. In this investigation Low also found that greater

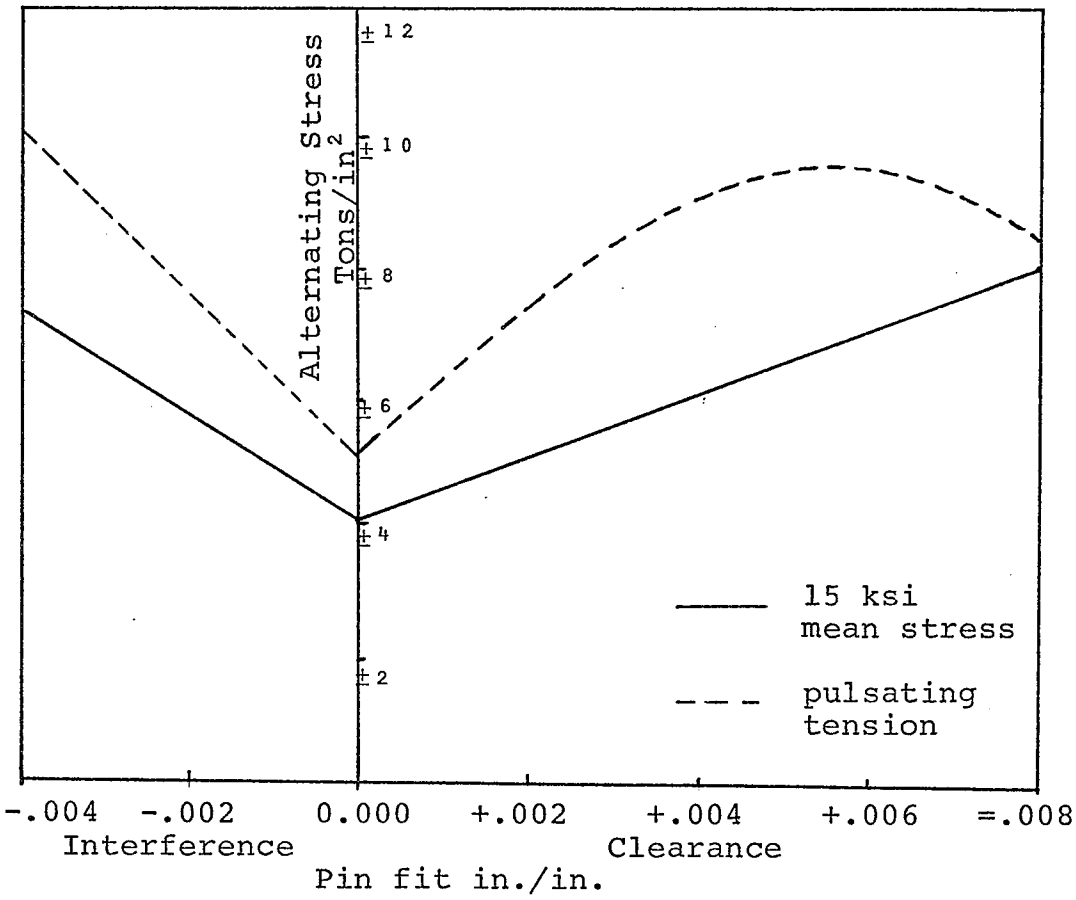

Figure 2.3. "Effect of pin fit on the endurance limit at 10^8 cycles", from White (10)

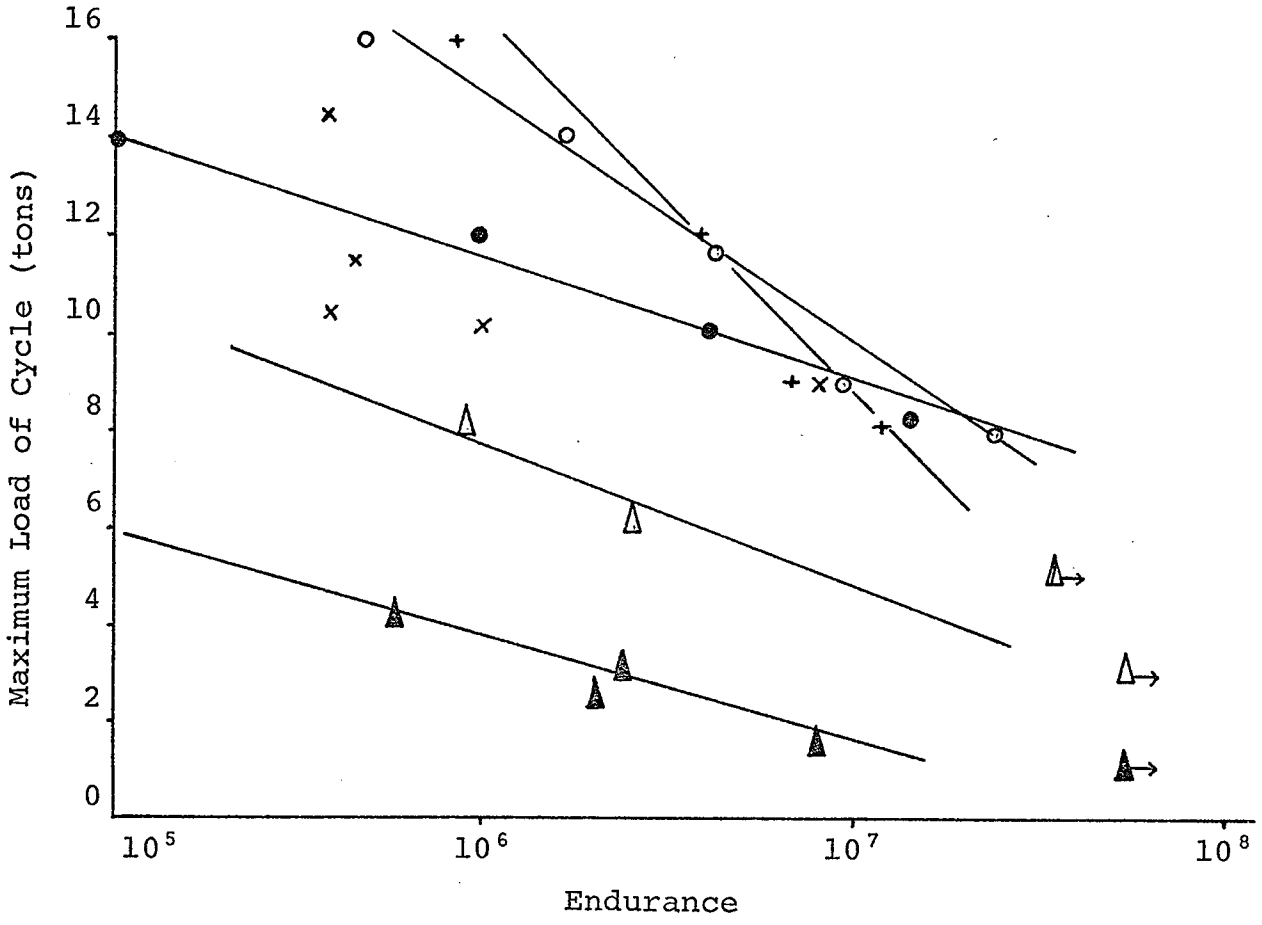

Figure 2.4. Effect of Interference, A. C. Low (4)

1 in. diameter pin

▲ .000	● 0.004	o 0.007	
△ .002	x 0.005	+ 0.010	in.

strengths were obtained with increased pin diameters. He also found that where shorter lives were called for, greater interferences were beneficial.

Mittenbergs and Beall (5) found somewhat lesser effects from interference in steels in axial tension plus bending. They obtained a twofold increase for .003 in. interference at 10^7 cycles where Low found a threefold increase for the same interference and life.

C. R. Smith (7) examined the taper-lok bolt, a variation of the interference fit bolt. These bolts proved to make significant improvements in unloaded holes but gains were only slight for loaded holes. Since failures invariably began through fretting at the washer edges interference was of little avail.

In circumstances where ease of assembly is an important factor interference bushings with exact fit pins may be used to obtain similar results to those for interference pins. A. C. Low (4) using 1 in. diameter bushings with .007 in. interference found strength improvements comparable to similar interference pins. C. R. Smith (6) investigated the effectiveness of hardened steel bushings in a 7075 aluminum alloy lug. Using a 1.25 in. nominal hole diameter two thicknesses of bushing wall and several degrees of interference were tried. The optimum improvement was with an interference of .006 in./in of hole diameter where the life was improved from 34,000 cycles

unbushed to greater than 10^6 cycles. McElhinney (3) found that in full scale wing fatigue tests, interference bushings lasted four times the life of interference pins.

Whaley (9) and later Speakman (8) investigated the effects on fatigue life of several methods of coining. Whaley, using 7075-T6 aluminum, pressed conical indentors of various pitch into the bolt hole openings. With the optimum pitch of 120° a threefold increase in fatigue life was found for low cycle fatigue. Whaley also investigated a method of pressing an annular region around the holes. With a narrow ring 1.5 times the hole diameter pressed to a depth of .025 ins., increased of up to 9.0 times the uncoined fatigue life were observed.

Speakman investigated similar types of coining which are illustrated along with those of Whaley in Fig. 2.5. Radius stress coining involved pressing the hole edges until a radius of .030 ins. was formed. Pad stress coining involved pressing an area surrounding the hole to a depth of .004 ins. Stress coin hole expansion consisted of plastically enlarging the bore of the hole to final size using a lubricated pin.

In all cases coining attempts to induce a residual compressive stress distribution around the hole and effectively lower the mean stress under loading. The residual stresses were thought to be of the order of the yield stress. Each type of coining is best suited to certain material

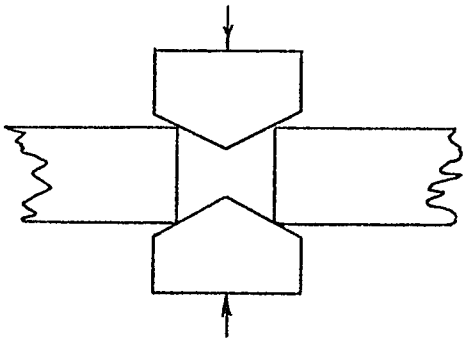

Conical Die Coining
Whaley

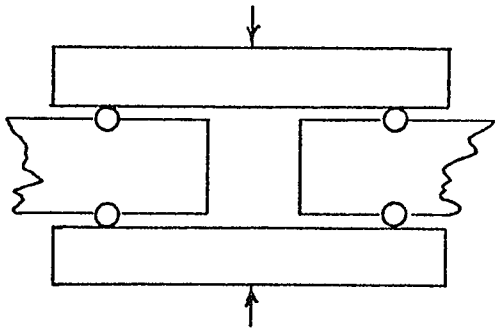

Ring Die Working
Whaley

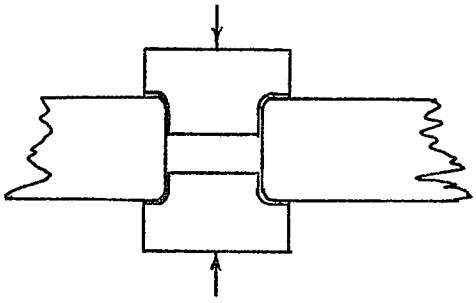

Radial Stress Coining
Speakman

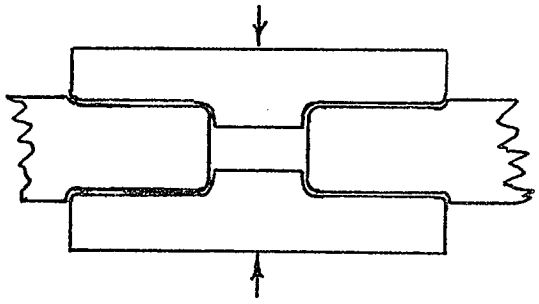

Pad Stress Coining
Speakman

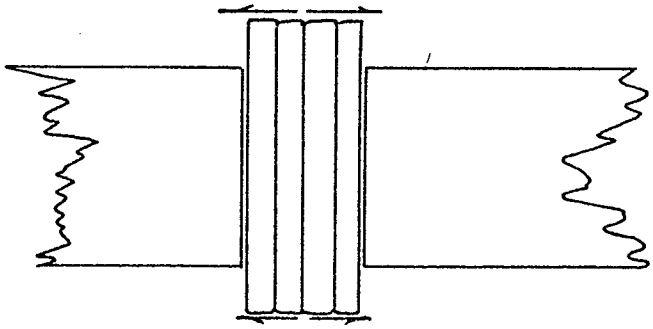

Stress Coin Hole Expansion
Speakman

Figure 2.5. Coining Methods described by Whaley (9) and Speakman (8)

thickness and bolt fit. Comparative data from Speakman's work may be found in Figs. 2.6 and 2.7.

White (10) investigated the use of a process called overstraining in which an oversized steel ball was forced through the bore of the hole plastically expanding it. Residual compressive stresses were formed along the bore and calculated to be as high as the yield stress. The fatigue strength of FV 520B steel lugs modified in this manner was found to be 1.6 to 1.8 times greater than that for unaltered lugs at 10^8 cycles.

Shot peening has been studied by a number of authors over the past forty years. By the hammering action of impinging steel shot the surface layer of an object is left in residual compression. This residually compressed layer approximately .020 ins. deep retards the nucleation and early stages of growth of fatigue cracks. Although this process was developed primarily for use with gear teeth and springs it has also been found beneficial for pin type connections. Mattson and Almen (2) studied the strengthening effects in connecting rods. Fatigue life improvements of over an order of magnitude were found for shot peened rods.

Strain peening is a slight variation of this technique where the part is prestressed during the peening operation. The resultant residual strains are much higher. Shot and strain peening are most effective for hardened steels.

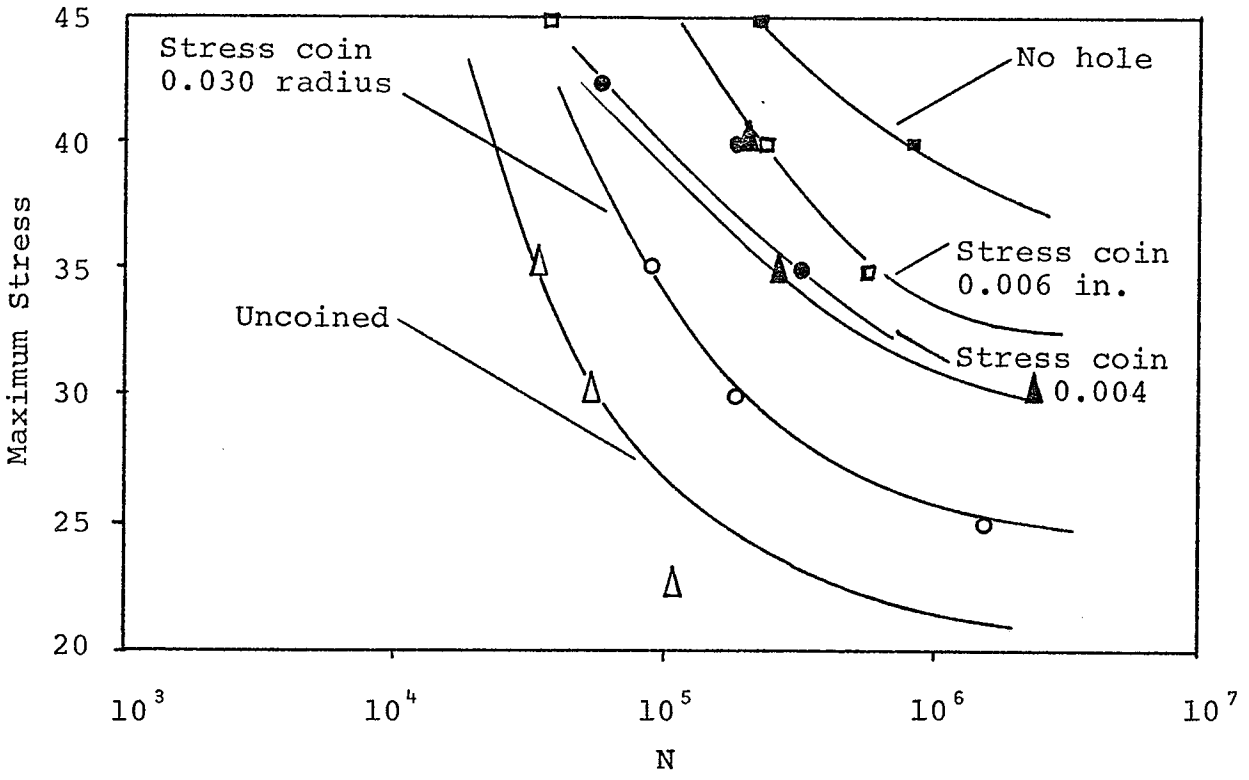

Figure 2.6. Fatigue test of 0.250 in. 2024-T351 nonclad aluminum by Speakman (8)

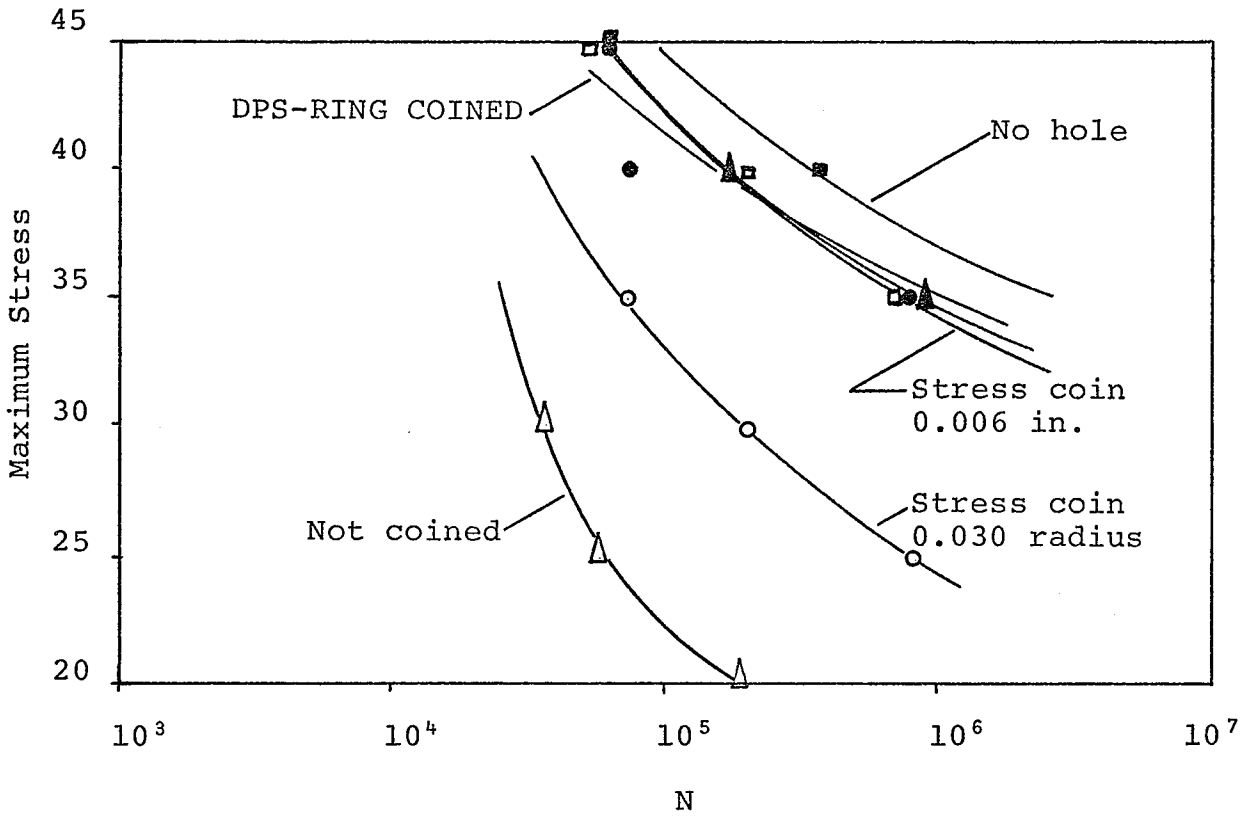

Figure 2.7. Fatigue test of .250 in 7075-T651 nonclad aluminum by Speakman (8)

Almen (2), White (10), and numerous other authors have investigated the effects of plating on fatigue strength. Depending on the plating material and method of application results vary from strength increases to decreases. Most commercial platings tend to decrease fatigue strength as they induce tensile residual strains at the surface.

Several diffusion hardening techniques have been successfully used to increase the fatigue strength of loaded holes and other stress concentrations. Carburizing and nitriding are the most common while White (10) used a "Sulphinuz" salt bath which adds nitrogen and sulphur to the surface, but of greater importance is the formation of residual compressive stresses in this surface layer through the resulting volume expansion. Benson (1) points out that this layer must be deep enough that it is well below the zone affected by stress concentrations from surface inclusions. In his study a method is presented that allows the selection of material and process variables to achieve the desired results for any surface.

Nelson, Ricklefs and Evans (74) studied the effects of heat treating on fatigue, comparing their results with those for shot peening. Steels of varying carbon content were subjected to a number of temper treatments followed by a water quench. The resulting compressive residual

stresses were measured for each case and the fatigue performance studies.

General studies of the fatigue strength of joints may be found in references (11) through (14). Also the role of residual stresses in structures under static and fatigue loading is abundantly described in references (15) through (31).

2.3 Synopsis

Each of the techniques mentioned attempted to improve the fatigue strength of loaded holes by reduction of stress concentrations and prevention of fretting. Clamping succeeded by providing an alternate path for load transmission. Interference and clearance fits approximately doubled the fatigue strength of lug connections, the former by increasing mean stresses while lowering alternating stresses, the latter by reducing fretting. The diffusion hardening, coining and overstressing techniques produce residual compressive stresses, acting to mitigate the stress concentration. Fatigue strength increases of from 1.5 to 2.0 were common. The effectiveness in fatigue strength improvement of the techniques discussed could roughly be ascertained through knowledge of their effectiveness in producing the desired beneficial prestress.

It must be noted that all tests were conducted under controlled laboratory conditions and that in actual practice many loading and fabrication variables will alter the effectiveness of any of the techniques.

Chapter 3

The Dimpling Process

3.1 Introduction

Chapter two outlined the efforts of researchers in past years to improve the fatigue strength of loaded holes through various fasteners, hardening or prestressing treatments. In this chapter a new method will be presented. This method which will be called the dimpling process, is employed to increase the fatigue strength of loaded holes in sheet material. It may be used in conjunction with pins, bolts, rivets or any of the common fasteners.

3.2 The Dimpling Process

The dimpling process effectively increases the fatigue strength of loaded holes by inducing residual compressive stresses around the hole. The process is best described by reference to figures 3.1 through 3.3. After locating the correct hole position the sheet is placed over a die and indented using a spherical or conical indentor as shown in Fig. 3.1. Next the area is flattened as shown in Fig. 3.2 between two smooth bars. Since some elastic springback occurs leaving a slight depression, a third operation completes the flattening by pressing the dimpled area with a low pitch cone as shown in Fig. 3.3. Several variations of dies and indentors were tried. They are outlined in chapter four, Table 4.2.

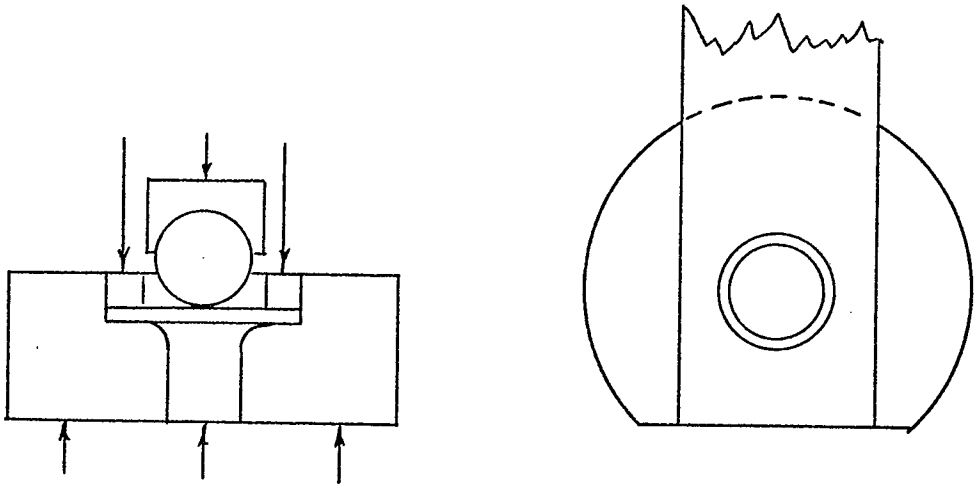

a) End View b) Top View

Figure 3.1. Indentation

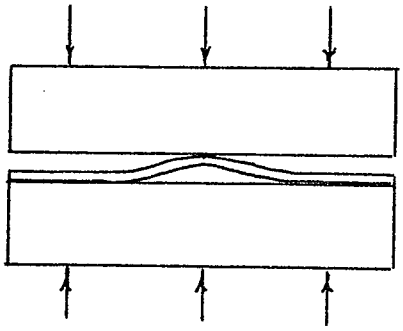

Figure 3.2. Flattening

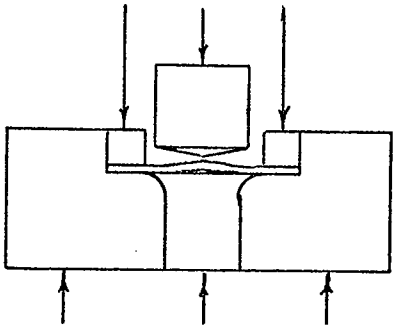

Figure 3.3. Returning of Elastic Springback

During the dimpling operation the indented material is plastically deformed, undergoing biaxial expansion accompanied by thinning. As the material is flattened it attempts to resume its previous position but since the area is now greater it is subject to constraining forces from the surrounding material. Some plastic deformation takes place and the mutual adjustment of dimpled and surrounding material induces residual elastic stresses with the net forces in each zone in balance. Even after the bolt or pin hole is drilled from the middle these residual stresses remain with magnitudes which may in theory reach the yield stress.

The process of dimpling is a simple one but, as far as a literature and patent search have revealed, a new one.

3.3 The Residual Stress Distribution

The dimpling process previously described results in the formation of residual elastic stresses surrounding a hole. These stresses may be linearly superposed with the service stresses provided their net value remains in the elastic range. Since the residual stresses at the edge of the hole are compressive, they act counter to the loading stresses, lowering the net value. The net residual plus elastic loading stresses are those which influence the fatigue strength of a specimen. Therefore, estimates of fatigue strength require a knowledge of the residual stress distribution.

The back-reflection x-ray diffraction technique was

used to measure the residual stress distribution on two forms of processed specimens. They were chosen on the basis of optimization fatigue testing described in chapter four. One form was dimpled using an 11/16 inch spherical indentor, the other using a 1/2 inch spherical indentor. The residual stress distributions as shown in Figs. 3.4 and 3.5 were determined from the x-ray stress measurements which are outlined in Appendix A.

A destructive strain gauge measurement technique was performed on the same specimens in an effort to corroborate the results. A complete description of these techniques with sample calculations is presented in Appendix A.

3.4 Prediction of Fatigue Strength from Residual Stresses

A new method for predicting the change in fatigue strength resulting from residual stresses will now be discussed. It will be applied in two cases where the dimpling process has been used on 2024-T3 aluminum, pin loaded, fatigue specimens described later in chapter four, section two. Predictions will be based on the nominal loading stresses and the residual stress adjacent to the hole. It will be assumed that all fatigue cracks leading to failures are nucleated at the hole edge.

A graphical technique is used for predictions. Beginning with a set of perpendicular axes, the mean stress forms the ordinate and the alternating stress forms the abscissa. A line representing the threshold stress level

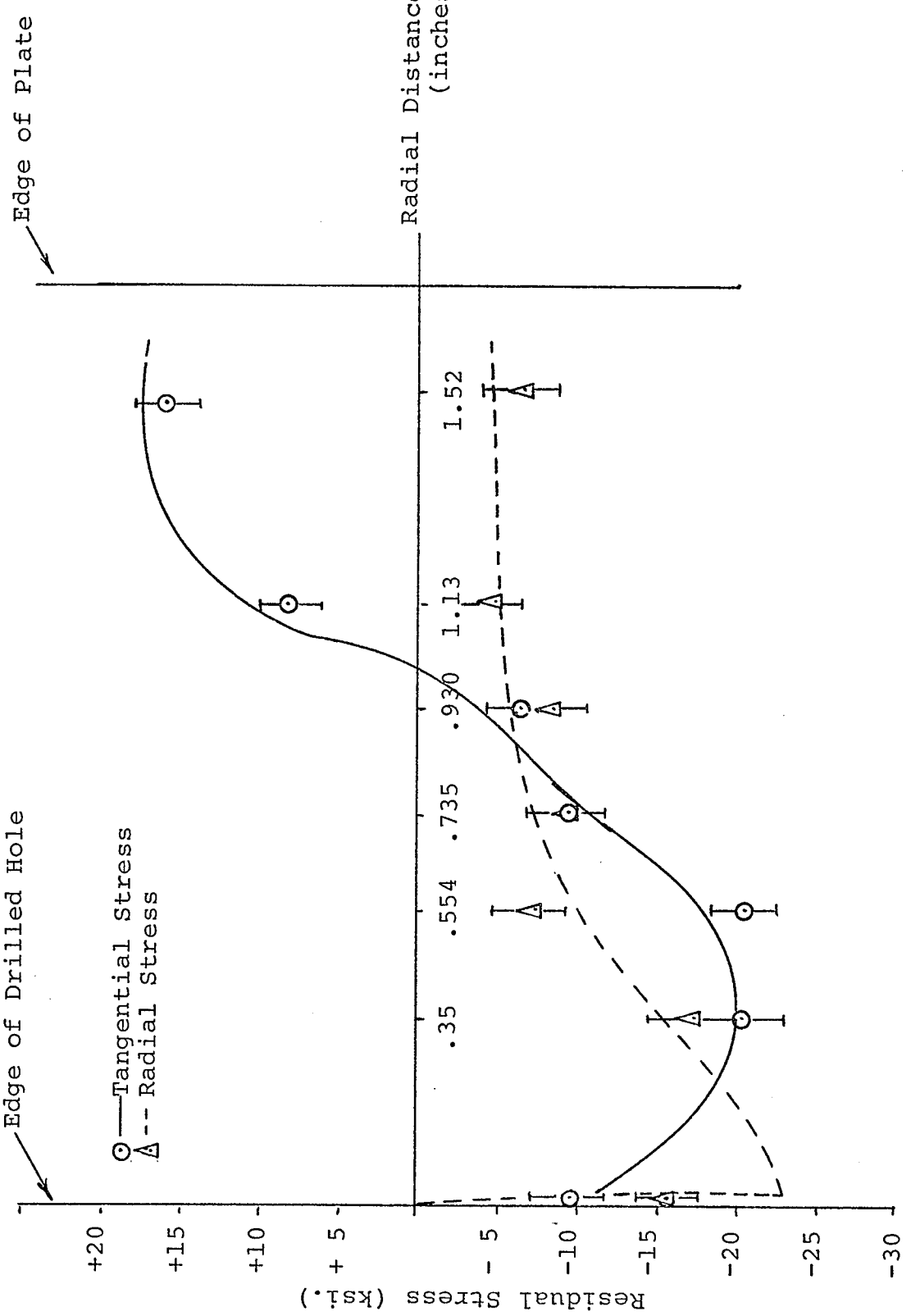

Figure 3.4. Residual Stress Distribution on a Series I Dimpled Specimen Determined by X-Ray Diffraction

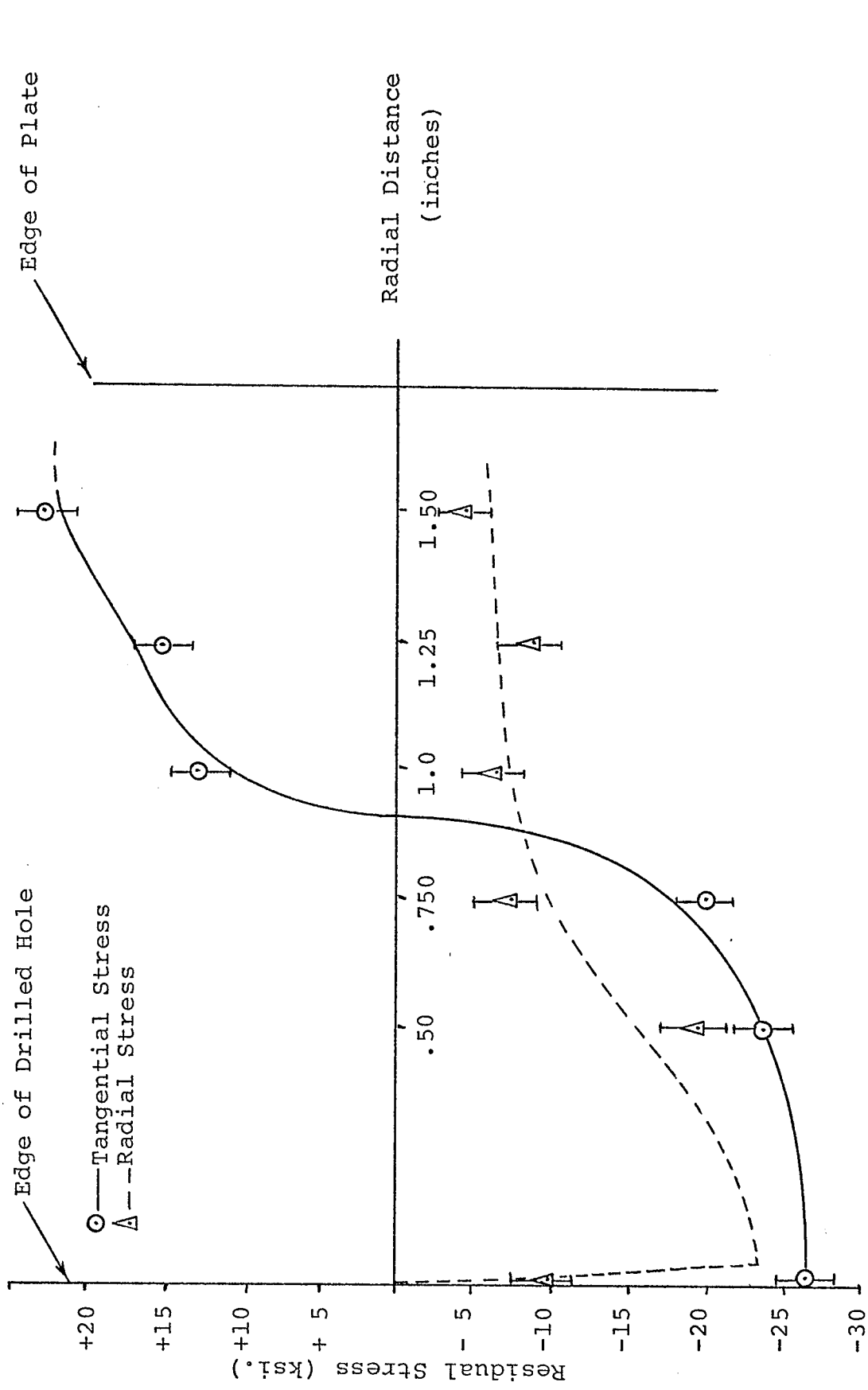

Figure 3.5. Residual Stress Distribution in a Series VIa Dimpled Specimen Determined by X-Ray Diffraction

for failure at a given number of cycles which is discussed in a paper by Fuchs (85), may be defined as:

$$S_a = (S_e - 0.5\ S_m)$$

where S_a = alternating stress, S_e = endurance limit and S_m = mean stress. This line is shown as the solid line AB in Fig. 3.6. From this it can be seen that for each value of mean stress there corresponds a value of alternating stress above which fatigue cracks will be nucleated and lead to failure. For the case where a stress concentration is present the position of this line may be shifted downwards by applying the correct factor K_f for the material:

$$S_a = \frac{1}{K_f} \quad (S_e - 0.5\ S_m)$$

The dashed line DE in Fig. 3.6 is an example of such a shift. It is seen to be a vertical translation only.

The position of the failure line for material with a stress concentration may also be determined from actual fatigue data. Here it is assumed that there are no non-propagating fatigue cracks and that crack nucleation leads to failure. The altered failure line differs from the plain material line only by translation along the vertical axis as previously described, so a single point suffices to establish its position. In Fig. 3.7 the unnotched failure line AB corresponding to a fixed service life is first drawn. From fatigue data on specimens with a stress concentration but no residual stresses the strength at

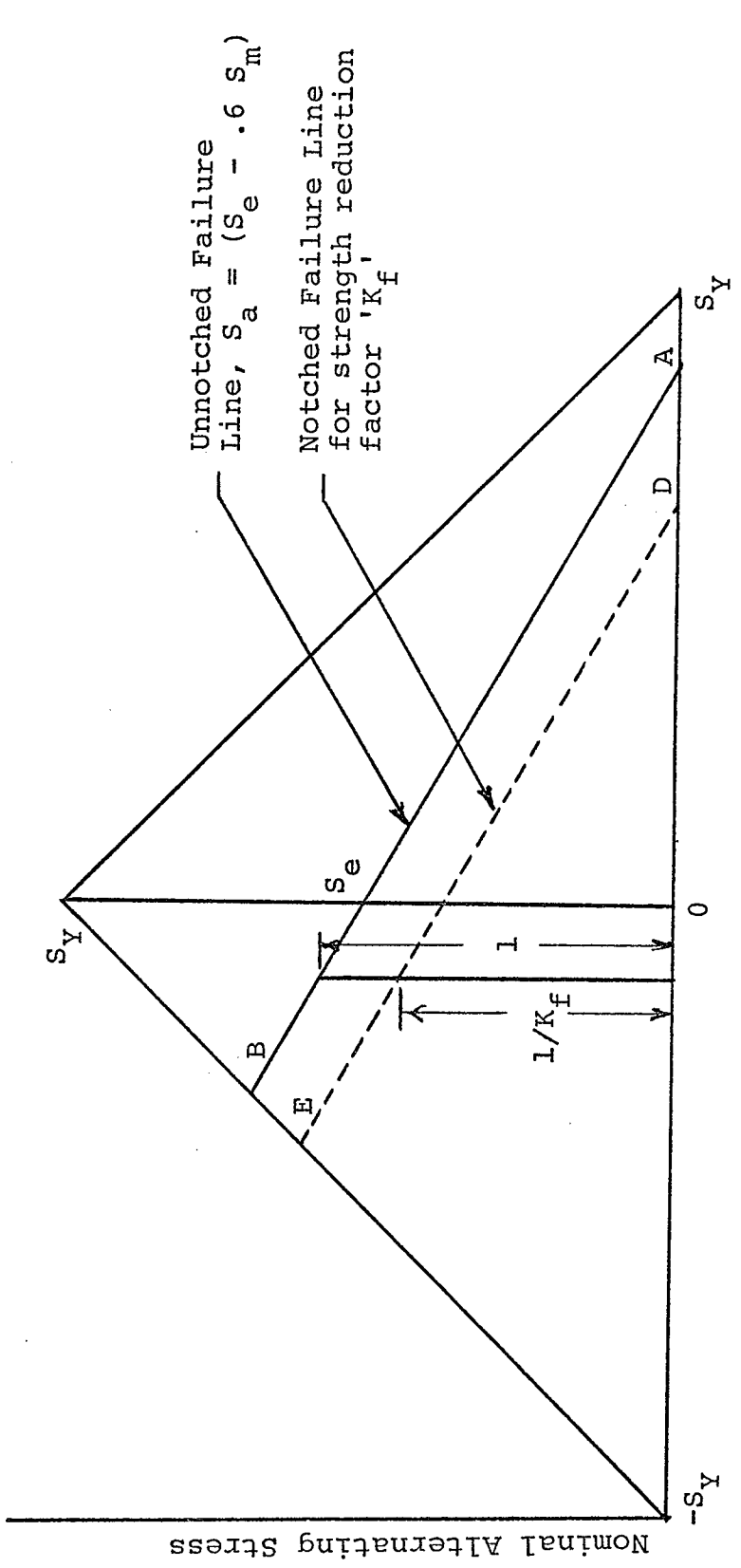

Figure 3.6. Graphical Method of Fatigue Strength Prediction

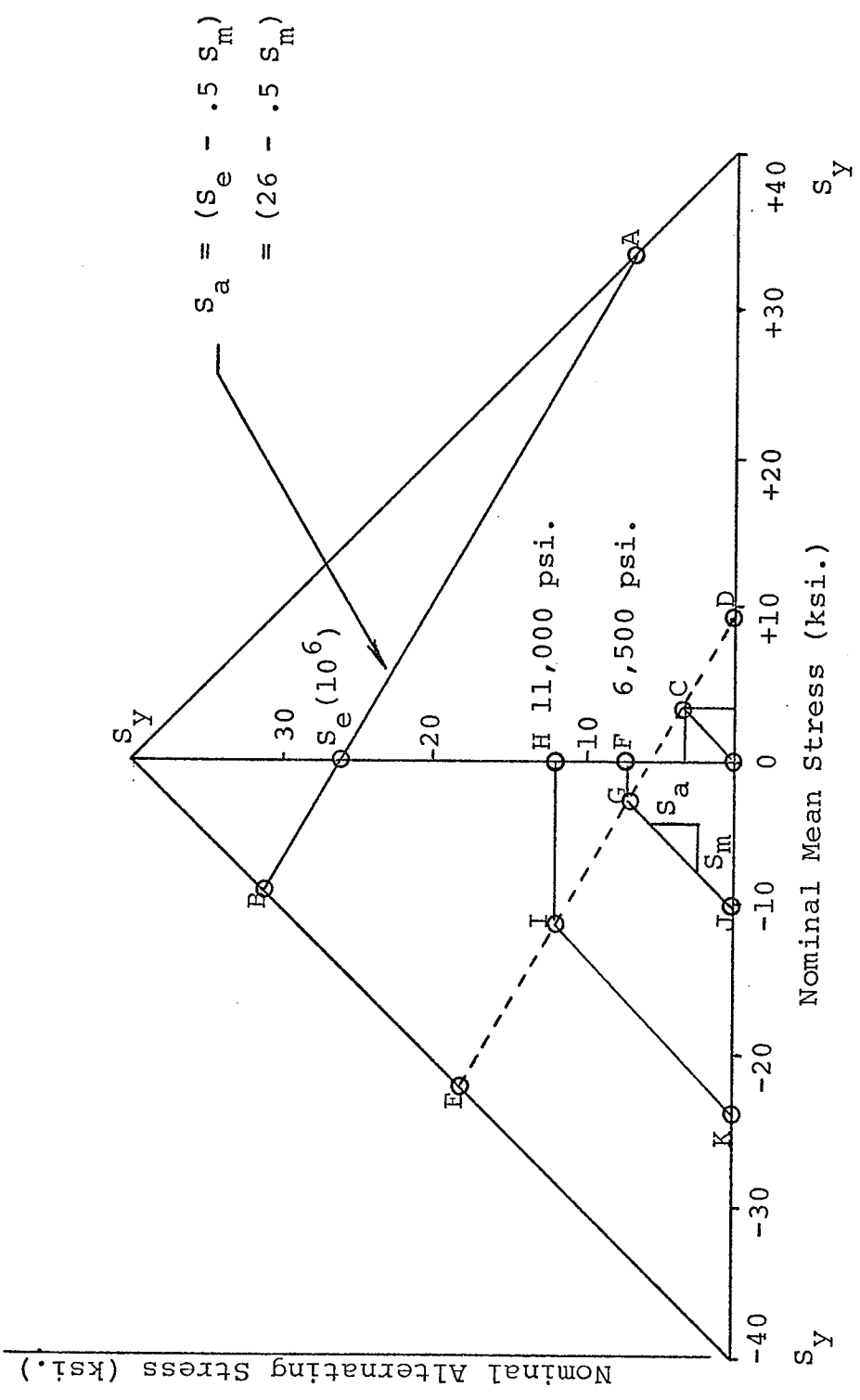

Figure 3.7. Prediction of Dimpled Fatigue Strength from Data on Undimpled Specimens

the fixed service life is determined and a corresponding point 'C' is placed on the diagram. Since this point lies on the failure line the notched line is a line DE parallel to the unnotched line passing through this point.

The change in fatigue strength due to the presence of residual stresses may be determined from the notched failure line. Residual stresses act as if they were statically applied external stresses superposed on to the loading stresses. They produce a shift in the mean stress level while leaving the alternating stress unchanged. In Fig. 3.7 this shift may be considered as a movement of the zero point on the mean stress axis by a value corresponding to the residual stress. To find the increase in strength, the desired ratio of the nominal alternating to nominal mean stress must be known. This will be referred to as the Load Ratio, S_a/S_m. A line of slope $S_a : S_m$ is then drawn from the new shifted origin to intersect with the notched failure line. The vertical coordinate 'F' of this intersection point 'G' is the maximum nominal alternating stress. The corresponding mean stress is computed from the Load Ratio S_a/S_m.

The above theory will now be used to predict the fatigue strength improvement of dimpled specimens. Predictions will be based only on the residual stresses measured by the x-ray technique for two forms of specimens as shown in Figs. 3.4 and 3.5. The failure line plotted in Fig. 7 is the correct one for 2024-T3 aluminum for an

expected life of 10^6 cycles. From fatigue data on identical undimpled specimens under pulsating tension the strength at 10^6 cycles is found to be approximately 3500 $\pm$ 3500 psi. The notched failure line is shown through this point 'C'. For the series I indentation the residual compressive stress is 10,000 psi and the origin is shifted by this amount to point 'J'. The loading again is pulsating tension with a Load Ratio of 1:1 and a line of 1:1 slope is drawn from the new origin to intersect the notched failure line at 'G'. The nominal alternating stress coordinate 'F' reads 6500 psi. The strength of a series I dimpled specimen at 10^6 cycles to failure should be 6500 $\pm$ 6500 psi. Similarly for a series VIa dimpled specimen with a residual stress of 25,000 psi the fatigue strength at 10^6 cycles should be 11,000 $\pm$ 11,000 psi.

The foregoing predictions were based on the assumption that cracks leading to failure were nucleated at the hole edge. Subsequent examination of failures indicated this to be true in all but a few instances. The predicted strengths are compared with actual fatigue data in chapter four, section three.

3.5 Use of a Brittle Lacquer to Determine the Residual Stress At a Hole Edge

To make simple predictions of the fatigue strength improvement it is necessary to know only the tangential

residual stress at the edge of the hole. However, x-ray diffraction stress measurements are time consuming and require expensive equipment. The necessary residual stress information can be obtained quickly and inexpensively using brittle lacquer and comparative tension tests on dimpled and undimpled specimens.

Brittle lacquer characteristically flakes at the yield stress and the load at which flaking just begins to occur can be recorded. Since residual stresses act as if superposed on the loading stresses, the yield point at the hole edge of the dimpled specimen is shifted by an amount corresponding to the residual stress level. Knowing the difference in yield load levels for dimpled and undimpled specimens the difference in stress at the hole edge, that being the residual stress, can be calculated. A description and sample calculations on a series VIa specimen may be found in Appendix B. The residual stress found in this manner was 19,200 psi. Such residual stress values may be used directly in predicting the fatigue strength of dimpled specimens.

3.6 Synopsis

The dimpling process of indenting then flattening sheet materials before hole drilling was found to induce residual compressive stresses around the hole balanced by residual tensile stresses at a distance away. The

nature of the stress distribution is shown in Fig. 3.4 and Fig. 3.5, which are plots of the stress at various points measured by the back reflection x-ray technique.

A technique was illustrated whereby, knowing the fatigue strength of an undimpled specimen, the loading, and the residual stresses at the hole produced by dimpling, the fatigue strength of a similar but dimpled specimen may be predicted.

A quick method of estimating the residual stress at the hole edge of dimpled specimens using comparative brittle lacquer-tension tests was described.

Chapter 4

Fatigue Testing of Dimpled Specimens

4.1 Introduction

A fatigue testing program was carried out to determine the effectiveness of the previously described dimpling process. In this chapter optimization fatigue tests on 2024-T3 aluminum are described which led to the selection of dimpling parameters for specimens undergoing x-ray analysis and subsequent S-N testing. Complete strength-life curves are plotted for undimpled specimens and two series of specimens dimpled according to the selected parameters. They serve to study relative changes in fatigue strength with cycles to failure and to verify strength predictions made in chapter three.

4.2 Fatigue Testing Program

1. Specimens

The specimens used for all fatigue tests were of commercially available 2024-T3 aluminum alloy sheet with alclad surfaces. They are illustrated in Fig. 4.1 while the chemical composition and physical properties of this alloy are listed in Table 4.1. The dimensions of all specimens were 1 x 5 x .050 ins. milled in batches of 40 to a tolerance of $\pm$ .002 ins. on the width. They were cut so that the direction of loading was transverse to that of rolling. Dies, shown in Fig. 4.2 and Fig. 4.3, were designed to fix specimens firmly and accurately in place

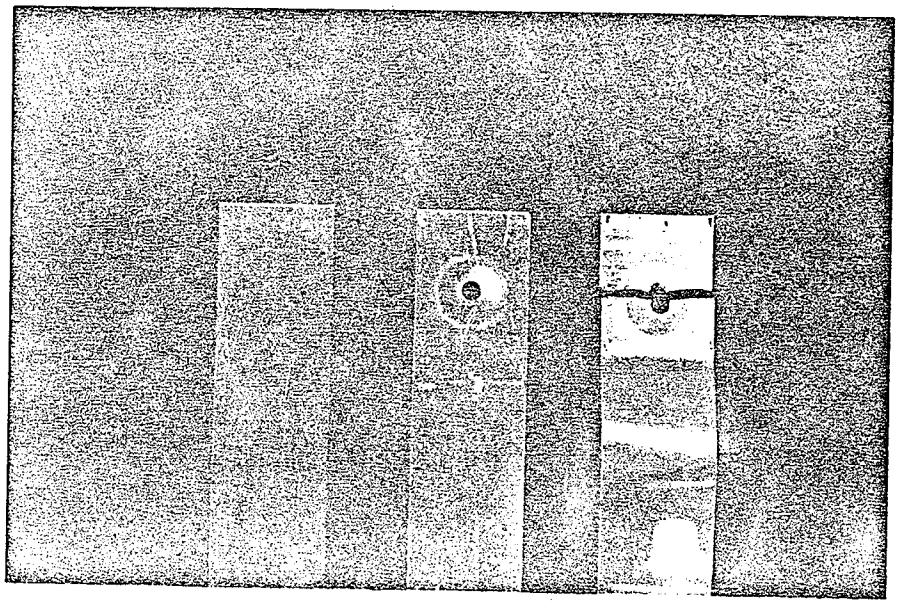

(a) (b) (c)

Figure 4.1. Fatigue Specimens (a) before dimpling (b) after dimpling, (c) after fracture

Table 4.1

Chemical and Physical Properties of
2024-T3 Alclad Aluminum Alloy Sheet

Chemical Properties

Cu	4.5 %
Mg	1.5 %
Mn	0.6 %

Physical Properties

Ultimate Tensile Strength	65,000 psi.
Yield Strength	45,000 psi.
Hardness	E 90-100
Fatigue Limit (unclad) @ 500 x 10^6 cycles R. R. Moore Rotating Bending	20,000 psi.
Modulus of Elasticity	10.6 x 10^6 psi.

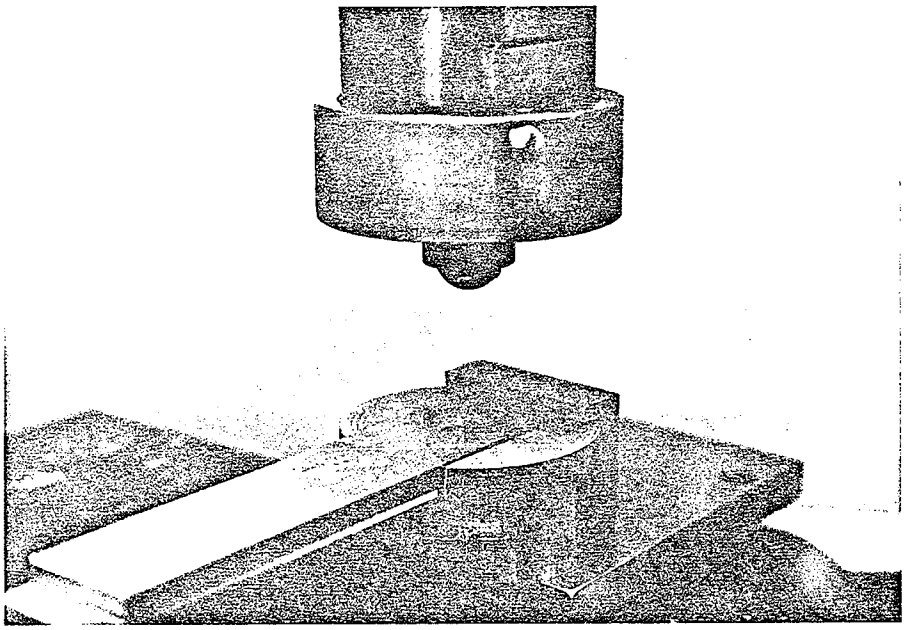

Figure 4.2. Die Used for Dimpling of Fatigue Specimens

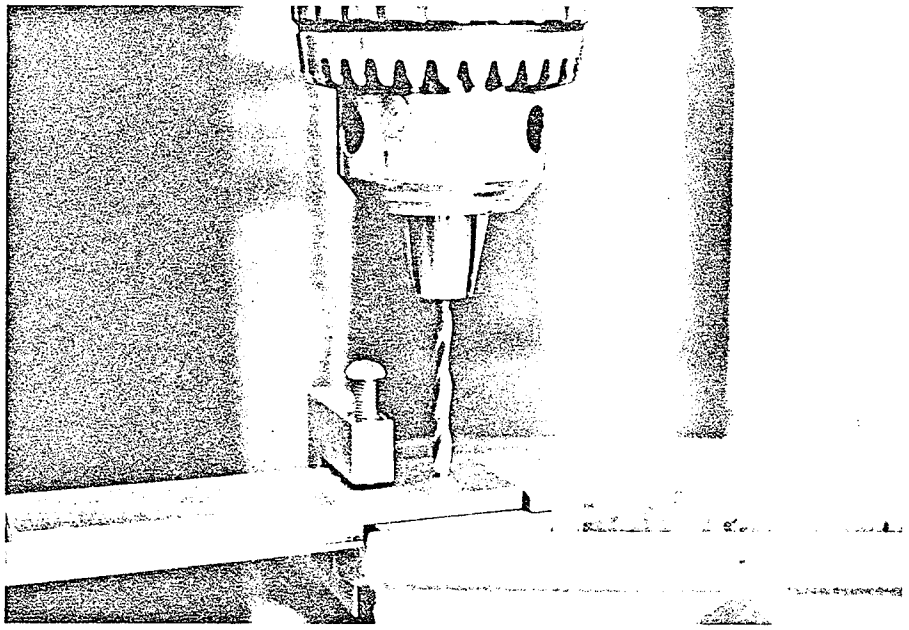

Figure 4.3. Die and Jig for Drilling of Fatigue Specimens

during both dimpling and drilling operations. The hole was drilled centrally within $\pm$ .002 ins.

Testing was conducted on a Baldwin-Lima-Hamilton model SF-1-U universal testing machine. The grips and loading clevis are shown in Fig. 4.4.

2. Optimization Testing

Fatigue tests to determine the influence of die size, indentor size and shape, and depth of indentation on fatigue life were conducted at a constant load level of 440 $\pm$ 420 pounds. Lives at this level fell in the range of 10^4 to 10^6 cycles to failure. Table 4.2 illustrates the range and combination of parameters investigated while test results are presented in Table 4.3. No single parameter played a dominant role in fatigue life improvement but general trends were apparent for each. Fatigue life increased with increasing die diameter, decreasing indentor diameter and increasing depth of indentation. The greatest life improvement was realized with a series VI die, a one-half in. spherical indentor and a depth of indentation of 0.100 ins. or two thicknesses of material. Specimens dimpled in this manner were referred to as series VIa specimens.

Series VIa specimens exhibiting the greatest life increases and series I specimens having intermediate life increases were selected for x-ray stress analysis described in Appendix A. The results of this stress analysis are presented in Figs. 3.4 and 3.5.

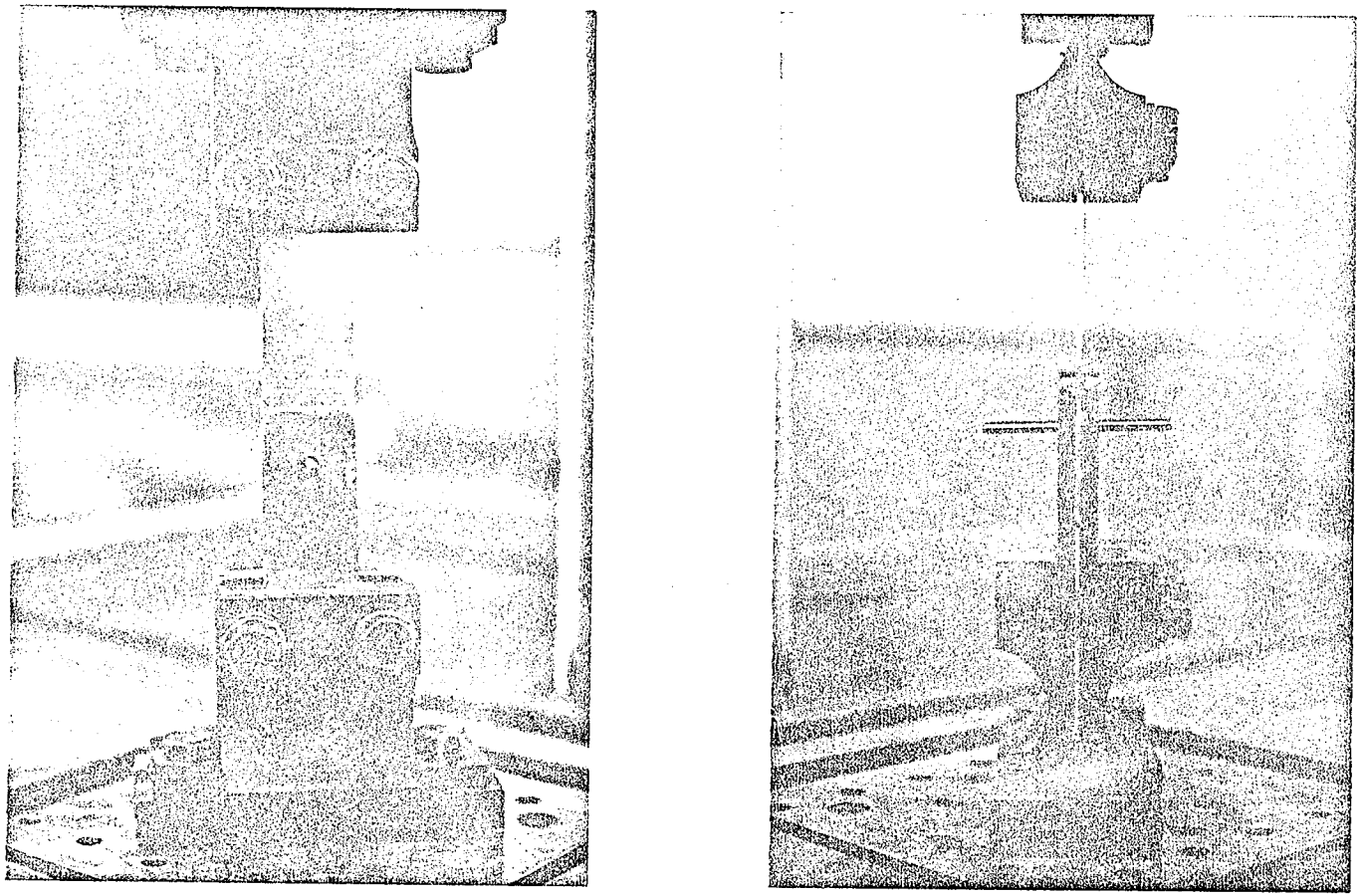

Figure 4.4. Grips and Loading Clevis for Fatigue Testing of 2024-T3 Aluminum Specimens

Table 4.2

Combinations of Dimple Parameters

Examined in Optimization Fatigue Testing

Die Series	Indentor				Depth of Indentation			
	1/2" Sphere 'SS'	11/16" Sphere 'LS'	Cone 'C'	Parabola 'P'	.025	.050	.075	.100
I		✓				✓		
II	✓						✓	
III	✓						✓	
IV a	✓					✓	✓	✓
b		✓				✓	✓	✓
c			✓		.040	✓		
d				✓	✓	.040	.060	
V a	✓					✓	✓	✓
b		✓				✓	✓	✓
VI a	✓					✓	✓	✓
b		✓				✓	✓	✓

Table 4.3

Fatigue Test Results for Dimple Parameter Optimization

Die Series	Indentor *	Depth of Indentention	Cycles to Failure
I	LS	.050	84,000/ 87,000/111,000/114,000
II	SS	.075	67,000/ 79,000/103,000
III	SS	.075	101,000/112,000
IVa	SS	.050	48,000/ 51,000/ 52,000
	SS	.075	92,000/ 97,000/112,000
	SS	.100	77,000/ 79,000/185,000
b	LS	.050	37,000/ 45,000/ 51,000
	LS	.075	55,000/ 87,000/ 99,000
	LS	.100	60,000/ 45,000/
c	C	.040	38,000/ 27,000
	C	.050	37,000/ 28,000
d	P	.025	45,000
	P	.040	76,000
	P	.060	240,000
Va	SS	.050	57,000/ 74,000
	SS	.075	145,000/ 93,000/144,000
	SS	.100	155,000/215,000/536,000
b	LS	.050	60,000/ 66,000
	LS	.075	79,000/278,000
	LS	.100	429,000/486,000
VIa	SS	.050	39,000/ 80,000
	SS	.075	130,000/170,000/206,000
	SS	.100	347,000/754,000/834,000
b	LS	.050	44,000/ 65,000
	LS	.075	74,000/328,000
	LS	.100	324,000/600,000
Undimpled			22,000/ 27,000/ 34,000

* SS stands for small (1/2 dia.) sphere,
LS for large(11/16 dia.) sphere, C for cone,
P for parabolic indentor

3. Strength-Life Fatigue Testing

To objectively study the dimpling effect full S-N fatigue testing curves were obtained for the following specimens:

1. undimpled
2. series I intermediate life improvement
3. series VIa maximum life improvement

A total of 102 specimens were used. Table 4.4 lists the results for each load level while a graphical presentation is made in Fig. 4.5.

4.3 Discussion

From the fatigue tests described it may be observed that the dimpling process produces substantial improvements in fatigue strength and that the degree of improvement depends upon the life to failure. The improvement may be predicted on the basis of measured residual stresses as will be discussed.

All forms of the dimpling process produced fatigue strength improvements. The level of improvement was determined by the magnitudes and distribution of residual stresses surrounding the loaded hole. This distribution was in turn governed by the relative deformation between the material elements, or the dimpled shape. Greater strength improvements were obtained with increasing die diameter up to $d/h = 4.40$, decreasing indentor diameter to $i/h = 3.08$ (where d = die dia., i = indentor dia., h = material thickness) and with increasing depth of indentation up to two thick-

Table 4.4

Fatigue Test Results for Undimpled, Series I Dimpled and Series VIa Dimpled Specimens

Load Level (lbs.)	Life (cycles to failure)			
Undimpled				
110 ± 100	2,462,000/2,483,000/2,394,000			
130 ± 120	1,091,000/1,533,000/1,586,000			
150 ± 140	872,000/1,176,000/	873,000/	749,000	
170 ± 160	527,000/	789,000/	870,000/	564,000
200 ± 190	247,000/	244,000/	283,000/	244,000
230 ± 220	150,000/	239,000/	145,000/	133,000
260 ± 250	130,000/	121,000/	131,000	
290 ± 280	94,000/	138,000/	88,000	
310 ± 300	92,000/	83,000/	84,000/	107,000
330 ± 320	99,000/	81,000/	72,000	
440 ± 420	22,000/	27,000/	34,000	
Series I Dimpled				
300 ± 280	920,000/2,580,000/1,020,000/1,020,000			
320 ± 300	777,000/	790,000/1,015,000/	994,000	
340 ± 320	703,000/	882,000/	957,000/	711,000
360 ± 340	474,000/	577,000/	650,000/	523,000
380 ± 360	409,000/	215,000/	226,000/	542,000
400 ± 380	175,000/	166,000/	169,000/	142,000
420 ± 400	115,000/	124,000/	113,000/	135,000
440 ± 420	87,000/	84,000/	114,000/	111,000
Series VIa Dimpled				
380 ± 360	1,450,000/	920,000/1,988,000/2,321,000		
400 ± 380	681,000/	520,000/	483,000/1,052,000	
420 ± 400	474,000/	680,000/	941,000/1,505,000	
460 ± 440	420,000/	842,000/	622,000/	501,000
480 ± 460	206,000/	101,000/	110,000/	122,000
500 ± 480	79,000/	66,000/	160,000/	189,000
520 ± 500	42,000/	48,000/	69,000/	120,000
540 ± 520	78,000/	44,000/	134,000/	77,000

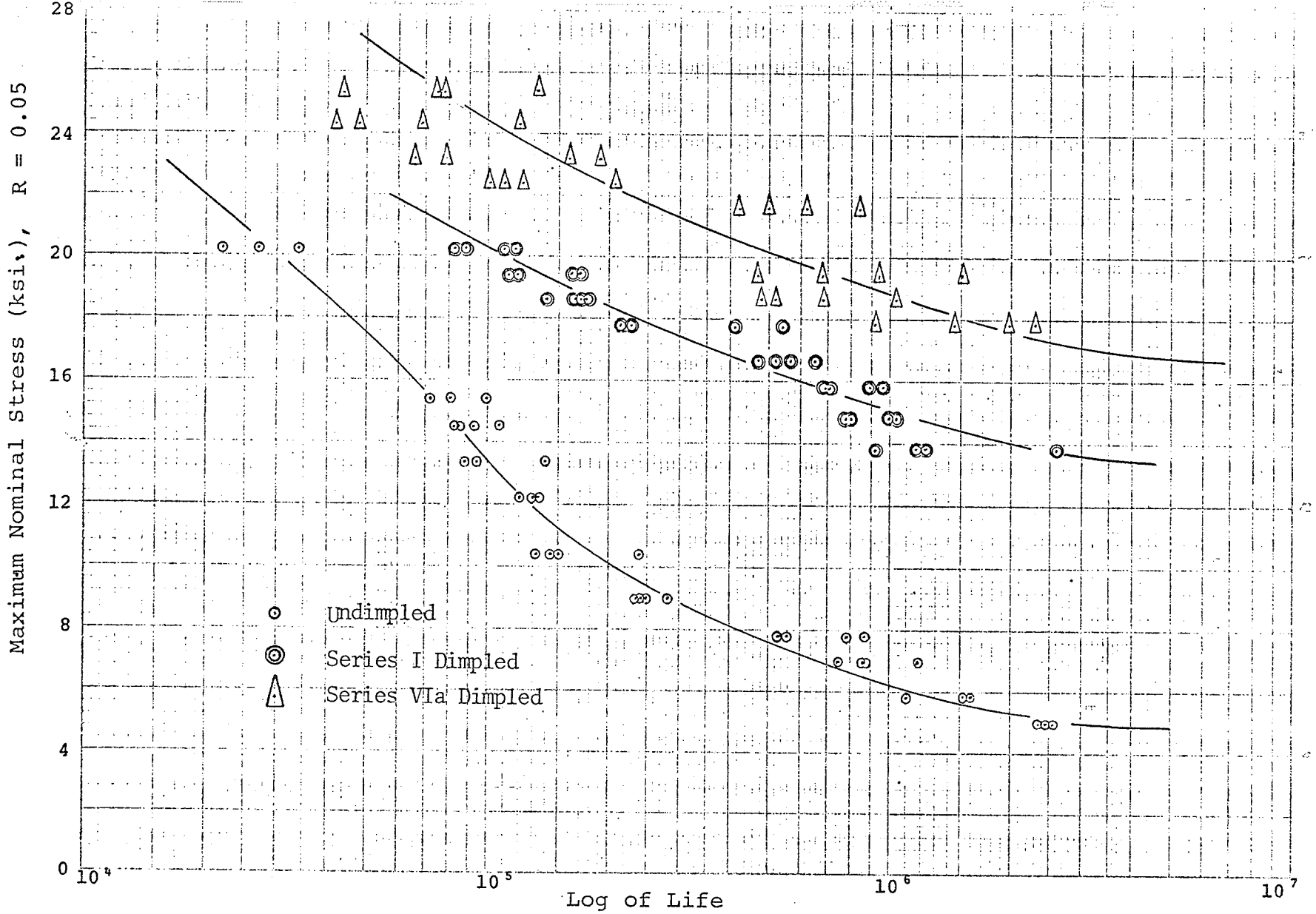

Figure 4.5. Results of Strength-Life Fatigue Testing

nesses. In other applications more suitable combinations than the series VIa may be found, depending on such physical limitations as proximity of adjacent holes, nearness to the sheet edge or thickness of the material. A rough guide may be - that the residual stress distribution should approximate a mirror image of the loading distribution with a slightly greater magnitude.

The S-N curves of Fig. 4.5 indicated that fatigue strength improvements were consistent for all lives, as the series VIa specimens at each point exhibited greater improvements than the intermediate form. However, the strength improvement ratios of both the series tested tended to decrease for shorter lives. This is in general consistent with all increases resulting from a shift in mean stress. For the case of residual stresses the decrease in improvement at shorter lives is even more pronounced since local yielding at higher loads may relieve the stresses.

The actual fatigue strength improvement ratios determined from the S-N curves for series I and series VIa specimens are compared in Table 4.5 to their corresponding values predicted in chapter three section four. The predicted values were based on the residual stress magnitudes. Since measurements of these stresses by the x-ray diffraction technique were precise only to within $\pm$ 1800 psi., the predictions suggest only the midpoint of a band of possible values. The width of the band is indicated to the right of the predicted values in Table 4.5.

Table 4.5

Comparison of Predicted vs Actual

Fatigue Strength Improvement Ratios

	Predicted Fatigue Strength Improvement Ratio	Actual Fatigue Strength Improvement Ratio
10^6 cycles		
series I	1.86 (1.70 – 2.14)	2.06
series VIa	3.14 (2.84 – 3.42)	2.86
10^5 cycles		
series I	1.46 (1.33 – 1.60)	1.41
series VIa	2.12 (1.89 – 2.26)	1.60

All the fatigue strength improvement ratios fell within their predicted band except that for series VIa st 10^5 cycles. It is believed that this discrepancy resulted from relaxation of the residual stresses due to yielding in the areas of high tensile stress. The addition of the loading stress to the residual stress at the edge of the series VIa specimen indicated a total stress of (25,000 + 25,400) 50,400 psi. This is in excess of the yield stress.

It appears from the reliability of the predictions which were within the bounds of fatigue test scatter and the accuracy of residual stress measurements that the fatigue strength improvements could be accounted for entirely in terms of a mean stress shift. Conversely, knowing the mean stress shift and the undimpled fatigue strength, the strength of dimpled specimens may accurately be predicted.

It is possible that supplementary effects may have been at work in altering the fatigue strength of dimpled specimens. Work hardening which accompanies any plastic deformation may have had either beneficial or adverse effects, likewise the relaxation of residual stresses. To understand and evaluate the dimpling process it was necessary to separate the roles of these contributing influences.

Work hardening occurred simultaneously with the plastic deformations necessary to produce residual stresses. It was therefore necessary to consult the literature for

tests separating the effects of work hardening on fatigue from other variables. Mattson and Roberts (70) using the process of presetting and strain peening found that work hardening had no effect on the fatigue strength of steel in unidirectional bending. Heywood (3) found no correlation between the fatigue strength of aluminum in axial tension and plastic working. These finds support indications in this thesis that the shift in mean stress as a result of compressive residual stresses was the prime influence on fatigue strength.

The relaxation of residual stresses was expected to detract to some degree from the beneficial effects of the dimpling process. Relaxation takes place as a result of either macroscopic yielding in some area or microscopic slip occurring with repeated loading. Relaxation caused by macroscopic yielding occurred at high load levels where the sum of the applied load and the residual tensile stresses exceeded the yield stress. The remaining residual stresses were distributed in the same manner but appreciably diminished. Relaxation also occurred as a result of microscopic slip which accompanies fatigue loading even in the stages between crack nucleation. However, researchers such as Morrow, Ross and Sinclair (72) suggest that unless macroscopic yielding occurs in the first few cycles of loading, predictions of fatigue strength may be based on the original residual stress distribution. Discussions of relaxation and the mutual influence of fatigue

loading on residual stresses and residual stress on fatigue may be found in references 65 through 80, 81 and 83 through 87.

To put the dimpling process in perspective it is desirable to compare its performance with that of the many other techniques discussed earlier. Table 4.6 compares the dimpling process with several processes which also induced compressive residual stresses around loaded holes. Evaluation of life increases were not generally possible since the tests in each study were performed at different stress levels. The fatigue strength improvement ratios given under the 'strength' column are the basis of comparison. These indicated that the coining techniques of Speakman which were also applied to aluminum alloys produced similar strength improvements. However, the dimpling process was tested on loaded holes while Speakman's tests were on free holes so that under equivalent conditions the dimpling process would appear to be superior. The processes of overstraining, sulfinuzing, peening and hardening all produced improvements in the range of SR equals from 1.5 to 2.25 with which the dimpling process compared favourably.

Table 4.7 compares the dimpling process with clamping, interference and clearance fits used to increase the fatigue strength of lugs. With the exception of Low's results, which showed incredible strength increases, the fatigue strength improvement ratios varied from 1.0 to 2.80 and were comparable to those for the dimpling process.

Table 4.6

Comparison of the Effectiveness of Fatigue Strength Improvement Techniques Employing Residual Stresses

	Loading	Strength	Life (cycles)
R. E. Whaley (9), Coining on 7075-T6 aluminum		S_{max} =	
a) 120° cone	Axial Tension	42,000 psi.	3.4x
b)	R = .1		9.6x
E. R. Speakman (8), Coining on aluminum alloys	Axial Tension		
a) Radius 2024-T3	R = .2	SR = 1.18	10^6
7075-T6		1.52	10^6
b) Ring Pad 2024-T3		1.41	10^6
7075-T6		2.00	10^6
c) Hole Expansion 2024-T3		1.50	10^6
avg..004-.006 7075-T6		2.00	10^6
D. J. White (10) on FV 520B steel	Axial Tension		
Overstraining			
a) Push fit pin	+ 9 ± 9 ksi.	SR = 1.8	10^8
	+15 ± 6.5	1.63	10^8
b) Clearance pin	+ 9 ± 9	1.8	10^8
	+15 ± 6.5	2.25	10^8
Sulfinuz	+ 8 ± 8	1.60	10^8
	+15 ± 6.5	1.63	10^8
Cadmium	+ 6 ± 6	1.2	10^8
	+15 ± 4	1.0	10^8
Mattson and Almen (2) shot peening on steel connecting rods	Axial Tension		10-20x
Horger (2) Quench hardening on steel drive shafts	Torsion	SR = 1.57	10^5
Roberts, dimpling on 2024-T3 aluminum	Axial Tension		
a) Series I	R = .04	SR = 2.06	10^6
b) Series VIa		2.86	10^6

Table 4.7

Comparison of the Effectiveness of Clamping, Clearance and Interference at Loaded Holes

	Loading	Strength	Life
D. J. White (10), on FV 520B steel	Axial Tension		
Interference			
0.000	+ 5 ± 5	SR = 1.0	10^8
	+15 ± 4	1.0	10^8
0.002	+ 7.5 ± 7.5	1.50	10^8
	+15 ± 5.5	1.38	10^8
0.004	+10 ±10	2.00	10^8
	+15 ± 7.5	1.88	10^8
Clearance			
0.002	+ 7.5 ± 7.5	SR = 1.50	10^8
	+15 ± 5.5	1.38	10^8
0.004	+ 9 ± 9	1.8	10^8
	+15 ± 6	1.5	10^8
0.008	+ 8.5 ± 8.5	1.7	10^8
	+15 ± 8	2.0	10^8
A. C. Low (4), on L65 aluminum	Axial Tension		
Interference			
0.000		SR = 1.0	10^6
		1.0	10^7
0.002		2.17	10^6
		3.83	10^7
0.004		3.28	10^6
		6.90	10^7
0.005		3.30	10^6
		6.50	10^7
0.007		4.24	10^6
		7.70	10^7
0.010		4.56	10^6
		6.50	10^7
Mittenbergs & Beall (5), on SAE 4340 steel	Tension + reversed bending	SR based on change in bending	
Interference			
0.000		SR = 1.0	15×10^6
0.0005		1.10	15×10^6
0.002		2.05	15×10^6
0.003		2.80	15×10^6

Table 4.7--Continued

	Loading	Strength	Life
Mittenbergs & Beall (5), on SAE 4340 steel Clamping 150 ft.-lb. 300 ft.-lb. 600 ft.-lb.	Tension + reversed bending	SR based on change in bending SR = 1.15 1.80 1.82	 $15x10^6$ $15x10^6$ $15x10^6$
C. R. Smith (6), on 7075-T6 aluminum Interference bushing 1/8" wall 0.000 0.005 0.0075 1/4" wall 0.005 0.0075 0.010	Axial Tension R = .015	S (nominal) = 18,800 psi.	 .85x 7.38x 31.50x 9.20x 28.60x 27.10x

The dimpling process appears to be an effective technique for increasing the fatigue strength of loaded holes. In sheet materials the process is quickly and easily applied producing superior strengths. However, for certain materials or for thick components the process is not suitable and one of the other techniques must be employed. Each of the techniques reviewed in this thesis is for certain applications the one most suitable. The dimpling process was designed to complement previous strengthening techniques providing high fatigue resistance in sheet materials where it is desirable to use the common fasteners.

4.4 Summary

Controlled load level fatigue tests indicated that substantial increases in the fatigue life of 2024-T3 aluminum specimens were obtained with all forms of the dimpling process while the greatest increase was for the series VIa process. Strength-life curves plotted for series I and series VIa specimens showed that fatigue strength improvement ratios increased with increasing life to failure. Also the strength improvements at 10^6 cycles were as predicted in chapter three within the range of fatigue test scatter and the accuracy of residual stress measurements.

Fatigue strength improvements for the dimpling process are comparable to those for previous improvement techniques described in chapter two. The dimpling process appears to be the best technique for sheet materials as superior strength improvements are attained.

Chapter 5

Summary and Conclusions

5.1 Summary

A new process for improving the fatigue strength of loaded holes was proposed. Several forms of this process, known as the dimpling process, were examined and representative specimens were fatigue tested to determine the most effective form.

The residual stresses were measured for series VIa, the most effective form, and series I, a less effective form. Predictions of the fatigue strength improvements were based on the mean stress shift resulting from the residual stresses measured.

Strength-life fatigue tests were conducted on series VIa and series I aluminum specimens to study the change in fatigue strength improvement ratios with life and to verify improvement predictions.

5.2 Conclusions

1) The dimpling process is effective in attaining high fatigue strength and life improvements in 2024-T3 aluminum sheet.

2) The degree of strength improvement is dependent on the magnitude and distribution of residual stresses left by the process around the loaded hole.

3) The degree of fatigue strength improvement may be predicted based on the tangential residual stress magnitude at the hole edge.

Bibliography

Fatigue Strength Improvement Techniques for Loaded Holes.

1. Benson, D. K., "Surface Treatments for Fatigue Strengthening," Achievement of High Fatigue Resistance in Metals and Alloys, ASTM STP 467 1970.

2. Fuchs, H. O., "Techniques of Surface Stressing to Avoid Fatigue," Metal Fatigue ed Sines and Waisman, McGraw-Hill 1959 pp. 197-232.

3. Heywood, R. B., "Designing Against Fatigue," Chapman and Hall, London, 1962.

4. Low, A. C., "The Fatigue Strength of Pin-Jointed Connections in Aluminum Alloy B.S. 65," Proc. Instn. of Mech. Eng., Vol. 172, No. 27, 1958.

5. Mittenbergs, A. A. and Beall, L. G., "Effects of Pin Interference and Bolt Torque on Fatigue Strength of Lug Joints," Proc. A.S.T.M., Vol. 63, 1963, pp. 671-683.

6. Smith, C. R., "Design Application for Improving Fatigue Resistance of Airplane Structures," Proc. A.S.T.M., Vol. 60, 1960, pp. 589-601.

7. Smith, C. R., "Interference Fasteners for Fatigue Life Improvement," S.E.S.A., Experimental Mechanics, Aug. 1965.

8. Speakman, E. F., "Fatigue Life Improvement Through Stress Coining Methods," Achievement of High Fatigue Resistance in Metals and Alloys, A.S.T.M., STP 467 1970.

9. Whaley, R. E., "Improvement in 7075-T651 Aluminum Alloy Fatigue Life by Coining," Proc. A.S.T.M., Vol. 63, 1963, pp. 692-705.

10. White, D. J. "Fatigue Strength of Small Pinned Connections Made From Alloy Steel FV 520B," Proc. Instn. of Mechanical Engineers, Vol. 182, No. 28, 1967-68.

11. A.S.M.E., "Metals Engineering - Design," ed O. J. Horger, McGraw-Hill, N.Y., 1953.

12. Grover, H. J., "Estimation of Fatigue Life of Welded Riveted and Bolted Structures," Metal Fatigue, ed Sines and Waisman, McGraw-Hill 1959, pp. 307-325.

13. Mann, J. H., "Fatigue of Materials," Melbourne University Press, 1967.

14. Smith, C. R. and Lindeneau, G. C., "Riveted Joints Fatigue Strength," A.S.T.M., Spec. Tech. Pub. 203 1956.

Residual Stresses.

15. Almen, J. L. and Black, P. H., "Residual Stresses and Fatigue in Metals," McGraw-Hill 1963.

16. A.S.M., "Residual Stresses," Metals Prog., Sec. Supplement to Metals Handbook, Vol. 68, 2A 1948, pp. 89-96.

17. Baldwin, W. M. Jr., "Residual Stresses in Metals," Proc. of A.S.T.M., Vol. 49, 1949, pp. 539-583.

18. Davidenkov, N. N. and Shevandin, E., "Research on Residual Stresses Developed in Bending," Journal Technical Physics (U.S.S.R.), Vol. 9, 1947, pp. 304-309.

19. Durelli, A. J., Jacobson, H. and Tsao, C. H., "Residual Stress Survey," Armour Research Foundation, Project 2-937 J, 1951.

20. Horger, O. J., "Residual Stresses," Handbook of Experimental Stress Analysis, ed. M. Hetenyi, Wiley, 1950, pp. 460-578.

21. Huang, T. C., "Bibliography on Residual Stresses," Special Publication 125, S.A.E., 1954.

22. Nachtman, E. S., "Residual Stresses," Machine Design, Dec. 1955, pp. 211-214.

23. Norton, J. T. and Rosenthal, D., "An Investigation of the Behavior of Residual Stresses Under Load and Their Effect on Safety," Welding Journal Research Suppl., Vol. 22, 1943.

24. Osgood, W. R., "Residual Stresses in Metal and Metal Construction," Reinhold Pub. Corp., New York 1954.

25. Queener, C. A. and De Angelis, R. J., "Elastic Springback and Residual Stresses in Sheet Metal Formed by Bending," A.S.M., Trans., Vol. 61, No. 4, pp.757-768, 1968.

26. Richards, D. G., "A Study of Certain Mechanically Induced Residual Stresses," Proc., Soc. Exp. Stress Analysis, Vol. 3, No. 1, pp. 40-61, 1945.

27. Richmond, W., "Residual Stresses in Metals," The Australasian Engineer, Vol. 43, pp. 21-29, 1943.

28. Sacks, G. and Espey, G., "Residual Stresses in Sunk Cartridge Brass Tubing," Trans., Amer. Institute Mining and Metalurgical Engineers, Vol. 147, pp. 74-88, 1942.

29. Waisman, J. L. and Phillips, A., Proc., Soc. Exptl. Stress Anal., Vol. 11, No. 2, p. 29, 1953.

30. Wilkins, C. A., "Internal Stresses of Metals," Metallurgia, Vol. 27, pp. 115-117, 1943.

31. Wilson, W. M. and Chao-Chien Hao, "Residual Stresses in Welded Structures," Welding Research Supplement, Journal, Amer. Welding Soc. Vol. 12, No. 5, pp. 295-320, 1947.

X-Ray Stress Analysis.

32. Barret , C. S., "X-Ray Analysis," Handbook of Experimental Stress Analysis ed M. Hetenyi, Wiley, 1950, pp. 977-1012.

33. Barret, C. S., and Massalski, "Structure of Metals," 3rd ed., McGraw-Hill, New York 1966.

34. Bolstad, D. A., and Quist, W. E., "The Use of a Portable X-Ray Unit for Measuring Residual Stresses in Aluminum, Titanium, and Steel Alloys," The Boeing Co., Airplane Division, Renton, Wash.

35. Christenson, A. L., "Measurement of Stress by X-Ray," S. A. E. Information Report TR-182, S.A.E. New York, 1963.

36. Colton, D. R., "The Effect of Magnetic Field on Interdiffusion in Dilute Aluminum-Copper Solid Sollutions," Ph.D. Thesis, University of Alberta, April 1964, P.63.

37. Cullity, B. D., "Sources of Error in X-Ray Measurements of Residual Stress," Journal of Applied Physics, Vol. 35, No. 6, June 1964.

38. Cullity, B. D., "Elements of X-Ray Diffraction," Addison Wesley, Reading, Mass., 1956.

39. Frommer, L. and Lloyd, E. H., "The Measurement of Residual Stresses in Metals by the X-ray Back Reflection Method with Special References to Industrial Components in Aluminum Alloys," Journal, Inst. Metals, Vol. 70, pp. 91-124, 1934.

40. Hayashi, Kosaburo, "X-ray Investigation of Lattice Strain and Deformation of Polycrystalline Metals," Ph.D. Thesis, Kyoto University,,Jan. 1970.

41. Kaufman, M., X-ray Lattice Strains in Plastically Deformed Metals," Ph.D. Thesis, University of California, Los Angeles, 1954.

42. Koistinen, D. P. and Morburger, R. E., Trans. ASM., Vol. 51, pp. 537-555, 1959.

43. Lynch, J. J. "The Measurements of Residual Stresses," Residual Stress Measurements, Americal Society for Metals, 1953.

44. Norton, J. T., "X-ray Methods in Field of Residual Stresses," Proc., Soc. Experimental Stress Analysis, Vol. 2, No. 1, 1944.

45. Norton, J. T. and Rosenthal, D., "Stress Measurement by X-ray Diffraction," S. E. S. A., Experimental Mechanics, Vol. 1, No. 2, 1943.

46. Norton, J. T. and Rosenthal, D., "Applications of the X-ray Diffraction Method of Stress Measurement to Problems Involving Residual Stresses in Metals," S.E.S.A. Experimental Mechanics, Vol. 1, No. 2, 1943.

47. Norton, T. J. and Rosenthal, D. and Maloof, S. B., "X-ray Diffraction Study of the Effect of Residual Compression on Fatigue of Notched Specimens," Welding Journal, Research Suppl., Vol. 25, P. 729, 1946.

48. Norton, J. T. and Rosenthal, D., "Recent Contributions to the X-ray Diffraction Method in the Field of Stress Analysis," Proc. S.E.S.A., Vol. 5, No. 1, 1947.

49. S.A.E., "The Measurement of Stress by X-rays," Sub. Committee on X-ray Procedures Div. 4 Res. Stresses, of the Iron and Steel Technical Committee, S.A.E., 1960.

50. S.A.E., "S.A.E. Handbook," 1964.

51. S.A.E., "S.A.E. Handbook," pp. 133-138, New York 1969.

52. Tangri, K. and Swaroop, B., "X-ray Studies on Residual Lattice Strains in Deformed Nickel," Met. Soc. of A.I.M.E., Trans., Vol. 245, No. 1, pp. 61-66, 1969.

Residual Stress Measurements.

53. Abuku, S. and Cullity, B. D., "A Magnetic Method for the Determination of Residual Stresses," Proc. S.E.S.A., Vol. 28, No. 1, May 1971-

54. Anderson, R. G. and Fahlman, E. G., "A Method of Measuring Internal Stresses in Brass Tubes," Journal, Institute of Metals, Vol. 32, pp. 367-383, 1924.

55. Birger, I. A., "Determining Residual Stresses in Samples with Irregular Shapes," Industrial Laboratory, Vol. 36, No. 1, pp. 105-110, Jan. 1970.

56. Kelsey, R. A., "Measuring Non-Uniform Residual Stresses by the Hole Drilling Method,"Proc. S.E.S.A., Vol. 14, No. 1, 1956.

57. Lake, B. R., Appl, F. J. and Bert, C. W., "An Investigation of the Hole-Drilling Technique for Measuring Planar Residual Stress in Rectangularly Orthotropic Materials," Proc. S.E.S.A., Vol. 27, No. 1, June 1970.

58. Meriman, J. L., de Garmo, E. P. and Johassen, F., "A Method for the Measurement of Residual Welding Stresses," Welding Journal, Research Suppl., Vol. 25, p. 340, 1946.

59. Rendler, N. J. and Vigness, I., "Hole-Drilling Strain Gauge Method of Measuring Residual Stresses," Proc. S.E.S.A., Vol. 23, No. 2, Dec. 1966.

60. Riparbelli, C., "A Method for the Determination of Initial Stresses," Proc. S.E.S.A., Vol. 8, 1950.

61. Vaidyanathan, S. and Finnie, I.,"Determination of Residual Stresses from Stress Intensity Factor Measurements," Journal of Basic Eng., Trans. A.S.M.E., paper No. 71 - Met. A.

62. Yarkovets, A. I. and Kiselev, N. M., "Measuring Residual Stresses in Thick-Walled Annuli of Small Diameter," Moscow Ordzhonikidze Aviation Institute translated by Zavodskaya Laboratoriya, Vol. 36, No. 11, Nov. 1970, pp. 1384-1386, 1971 Consultants Bureau, Plenum Publishing Corp., N. Y.

63. Yen, S. W., "Computer Solutions of Stress Distribution at a Hole Due to Stress Coining and Loads," Report DAC-67515 Douglas Aircraft Company, March 1969.

64. Zapel, E. J., "Method of Determining Residual Stresses in a Biaxial Stress Field," Proc. S.E.S.A. Vol.19, No. 2, 1962.

Residual Stresses in Fatigue.

65. Dolan, T. J., "Residual Stress, Strain Hardening and Fatigue," Internal Stresses and Fatigue in Metals, ed Rassweiler and Grube, Amsterdam, 1959.

66. Dugdale, D. S.,"Effect of Residual Stress on Fatigue Strength," Welding Research Supplement, Welding Journal, Vol. 38, #1, Jan. 1959.

67. Felgar, R. P., "Effect of Shot Peening on Fatigue Strength," A.S.M.E. paper No.58-SA-46, 1958.

68. Fuchs, H. O., "Forecasting Fatigue Life of Peened Parts," American Society for Metals, Metals Progress, May 1963.

69. Mattson, R. L. and Coleman, W. A., "Effect of Shot Peening Variables and Residual Stresses on the Fatigue Life of Leaf Spring Specimens," S.A.E. Trans., Vol. 62, 1954, p. 546.

70. Mattson, R. L. and Roberts, J. G., "The Effect of Residual Stresses Induced by Strain Peening Upon Fatigue Strength," Society of Automotive Engineers, Trans. Vol. 68, 1960, pp. 130-136.

71. Morrow, J. and Sinclair, G. M. "Cycle-Dependent Stress Relaxation," A.S.T.M., Spec. Tech. Pub. 237, Philadelphia, 1958, pp. 93-109.

72. Morrow, J.,Ross, A. S. and Sinclair, G. M., "Relaxation of Residual Stresses due to Fatigue Loading," Society of Automotive Engineers, Transactions, Vol. 68 1960, pp. 40-48.

73. Morrow, Jo Dean and Millan, J. F., "Influence of Residual Stresses on Fatigue of Steel," S.A.E. Handbook Supplement T R-198, S.A.E. New York, July 1961.

74. Nelson, D. V., Ricklefs, R. E. and Evans, E. P., "The Role of Residual Stresses in Increasing Long Life Fatigue Strength of Notched Machine Members," Achievement of High Fatigue Resistance in Metals and Alloys, ASTM, STP 467, American Society for Testing and Materials, 1970.

75. Peterson, E. W., "The Role of Stress Distribution in Fatigue," The William M. Murray Lecture Society for Experimental Stress Analysis, Vol. 18, No. 1, Apr. 1961, pp. 105-115.

76. Rosenthal, D., Sines, G. and Zizicas, G., "The Effect of Residual Compression on Fatigue," Welding Journal, Research Suppl., Vol. 28,p.98, 1949

77. Richards, D. G., "Relief and Redistribution of Residual Stresses in Metals," Residual Stress Measurements, A.S.M. 1952.

78. Rosenthal, D. and Sines, G., "Effect of Residual Stress on the Fatigue Strength of Notched Specimens," Proceedings, A.S.T.M. Vol. 51, 1951, pp. 596-609.

79. Rosenthal, Daniel, "Influence of Residual Stresses on Fatigue," Metal Fatigue, ed Sines and Waisman, McGraw-Hill, 1959, pp. 170-197.

80. Ross, A. S. and Morrow, J., "Cycle-Dependent Stress Relaxation of A-286 Alloy," Trans. A.S.M.E. Vol. 82, Sept. 1960.

Fatigue

81. Evans, W. P. and Millan, J. F., "Effects of Micro-strains and Particle Size on the Fatigue Properties of Steel," S.A.E. paper 793B, Society of Automotive Engineers, New York, Jan.1964.

82. Faires, V. M., "Design of Machine Elements," Macmillan, New York, 1965.

83. Forrest, P. G., "Fatigue of Metals," Pergamon Press, New York, Addison-Wesley, Reading, Mass. 1962.

84. Forsyth, P. J., "The Physical Basis of Metal Fatigue," American Elsevier Pub., New York 1969.

85. Fuchs, H. O., "A Set of Fatigue Failure Criteria," A.S.M.E., Vol. 87, pp. 333-343, June, 1965.

86. McClintock, F. A. and Argon, A. S., "Mechanical Behaviour of Materials," Addison-Wesley, Reading, Mass. 1966, pp. 420-442.

87. Harris, W. J., "Metallic Fatigue," London 1961.

Appendix A

Measurement of Residual Stresses

A.1 The X-ray Diffraction Technique

Measurement of strains by x-ray diffraction relates more than any other technique to the fundamental definition of elastic strain. This is said because the gauge length over which elastic deformations are measured is actually a material's interatomic lattice spacing. Since plastic strains are a result of planar slip they have no effect on this parameter and are not measured. With only elastic strains measured this technique is ideal for 'residual stress' measurement where the elastic strains must be separated from plastic strains. A unique advantage of the x-ray diffraction technique is that strains may be measured while the material is in the stressed state. The technique is thus non-destructive since it does not require that samples of material be removed to obtain 'unstressed' readings. A further advantage of the x-ray technique is that high stress gradients may be measured. The incident x-ray beam is collimated to about 1 m.m. in diameter so that the stresses measured approach those for a single point.

Despite these advantages there are a number of limitations placed on the technique by the particular materials upon which measurements are taken. The technique relies on the reflection of the x-ray beam by a number of

suitable oriented lattice planes. It is necessary that a number of grains contribute to the reflection. Since the beam is small the material must have a fine grain size. As illustrated in Fig. A.1, large grained materials produce a spotty diffraction pattern which is not readily measurable. Cold worked material presents a measuring difficulty since gross plastic strains also leave microstrains between unequally deformed grains. The diffraction pattern of a cold worked material is broad, hazy and difficult to measure.

The penetration of x-rays varies with materials but even for soft materials it is only of the order of several thousandths of an inch. Since the measurements are taken virtually at a free surface all non-planar stresses are zero and all measured strains are biaxial.

For a detailed discussion of x-ray diffraction and its use in residual stress measurements references 32 through 52 may be consulted. Other techniques for residual stress measurement are described in references 53 through 64.

A.2 The Three-Shot Back Reflection Method

The three shot back-reflection technique is used for measuring the two principal stresses on a surface when their directions are known. The apparatus is illustrated in Fig. A.2 and Fig. A.3. It consists of an x-ray source, a collimator constricting the rays to a beam 1 mm. in diameter, a film plate held in a suitable cassette

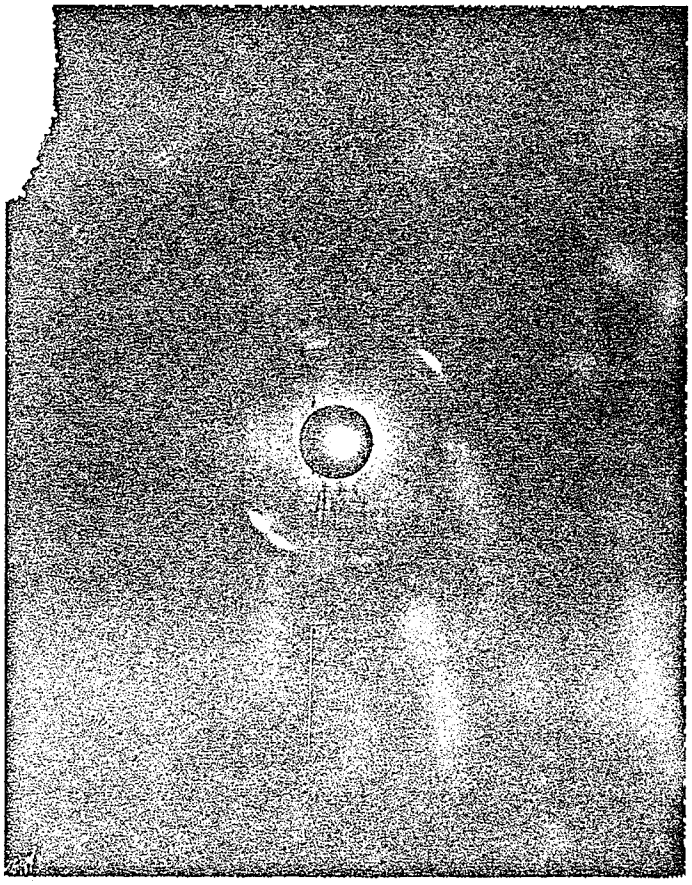

Figure A.1. Spotty Diffraction Pattern of Large Grained Material

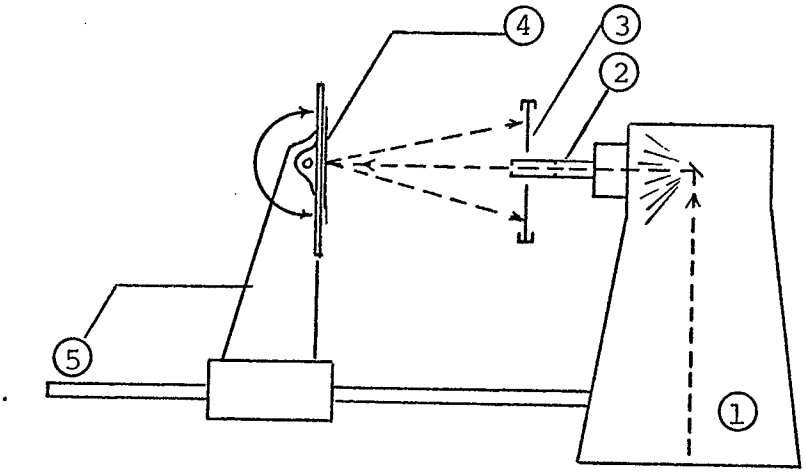

Figure A.2. X-ray Apparatus (side)

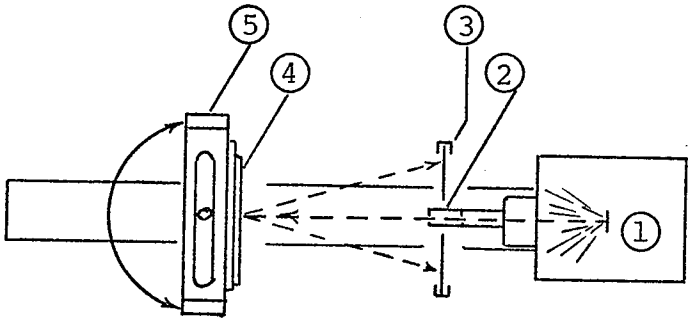

Figure A.3. X-ray Apparatus (top)

① x-ray source
② collimator
③ film casette
④ specimen
⑤ bi-planar rotating specimen holder

perpendicular to the x-ray beam, and a specimen fixture to adjust the position and angle of incidence of the beam on the specimen surface.

The collimated beam strikes the specimen and is diffracted by lattice planes according to the Bragg Law:

$$n\lambda = 2d \sin\theta$$

where 'n' is an integer describing the order of reflection, 'λ' is the wave length of incident radiation, 'd' is the material lattice parameter and 'θ' is the angle of incidence. The reflected beam intersects the film as a series of spots occupying positions on one or more coincident circles as shown in Fig. A-4. Each of these circles is a reflection from some particular set of planes with a common spacing 'd'. One of the circles is chosen for strain measurement which requires that its diameter be determined. To fascilitate this measurement the film may be oscillated $\pm$ 10^{o} to 15^{o} so that the spots are smeared together to form a complete circle. Researchers such as Norton and Rosenthal (45) and Barret (33) have found that such small oscillations introduce negligible errors.

From the Bragg Law it may be noted that a change in 'd', the lattice parameter, will, for a certain wave length 'λ', result in a change of 'θ' the angle of diffraction. Referring to Fig. A-5, changes in 'θ' are reflected in a change in the diameter of the circle formed by the

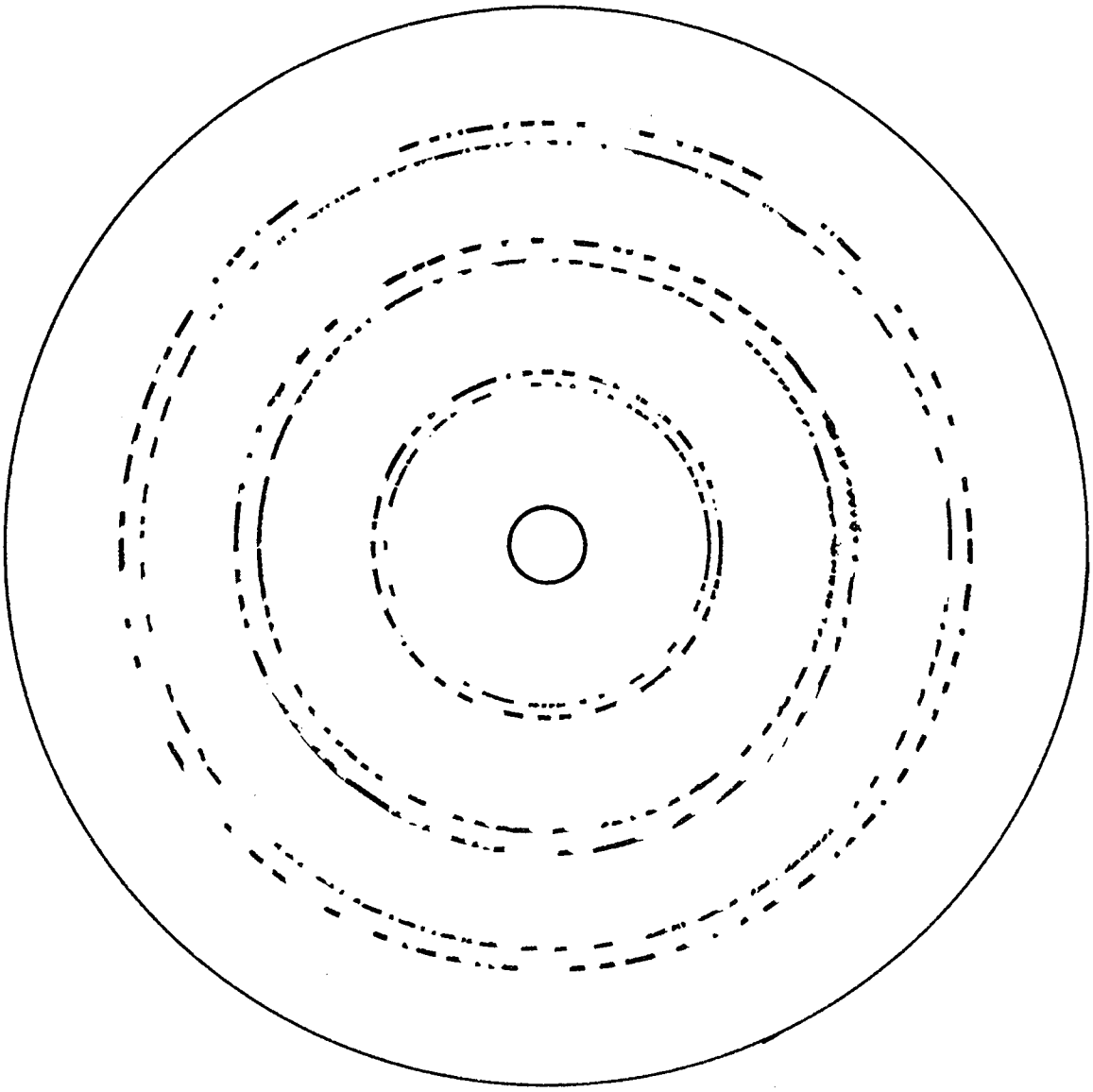

Figure A.4. Diffraction Pattern with Film Held Stationary

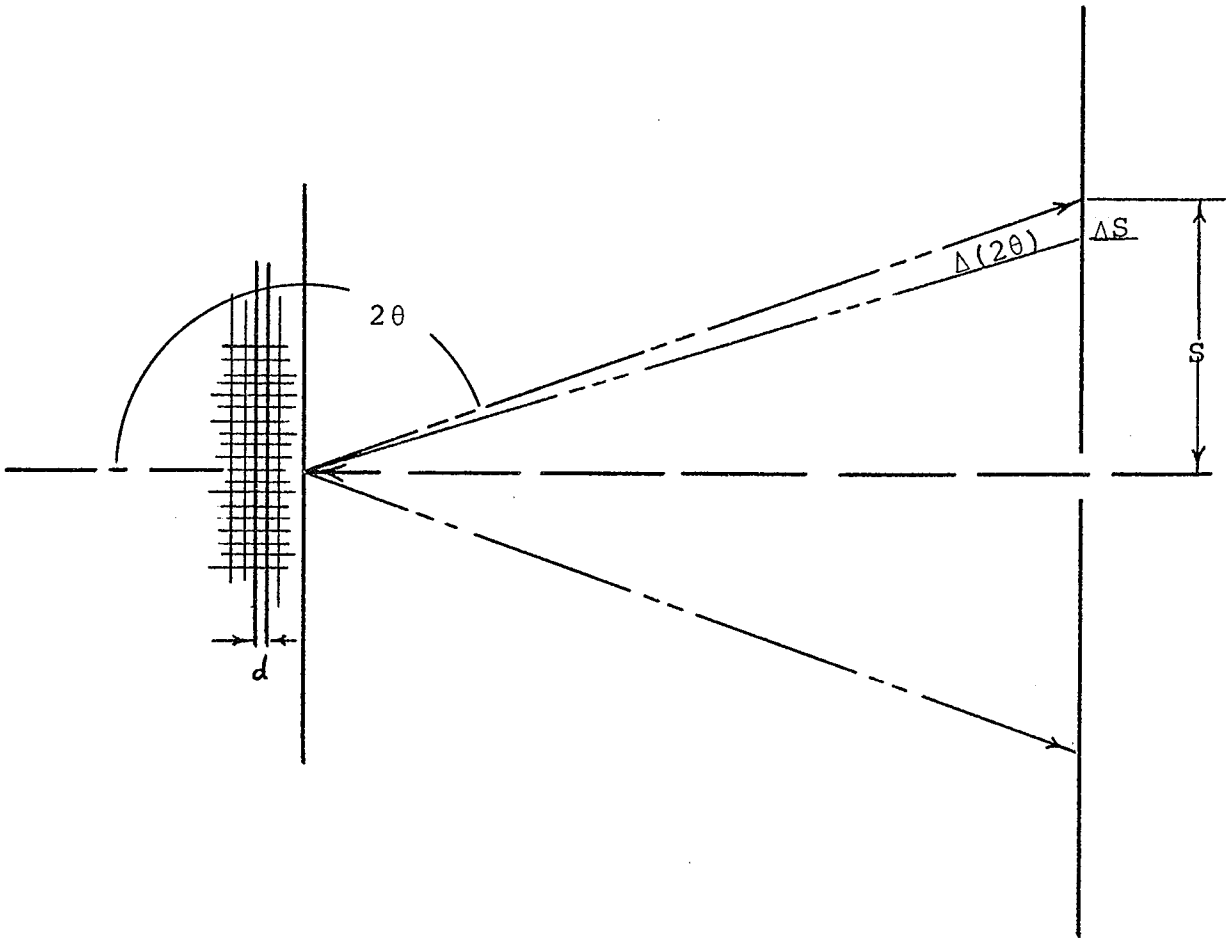

Figure A.5. X-ray Beam Diffraction

diffracted beam. Hence measurement of the diameter of the circle is an indication of the strained lattice parameter.

The determination of the two principal stresses requires three x-ray shots; one perpendicular to the surface and the other two inclined at 45^{o} to the surface, oriented in the directions of the principal stresses. The specimen to be measured in this case was mounted on a plate capable of rotation about both the horizontal and vertical axes. The beam struck the specimen at the pivot point so that the specimen to film distance remained constant.

The first shot, taken at normal incidence is illustrated in Fig. A-6 and A-7. The strain measured is that perpendicular to the surface or:

$$\varepsilon_3 = \varepsilon_z = \frac{\Delta l_z}{l_z} = \frac{d_n - d_o}{d_o}$$

d_n = normal lattice parameter, strained

d_o = unstrained lattice parameter

The second and subsequent shots are taken at some azmuthal angle'ϕ'corresponding to a principal direction, inclined at some angle'ψ'(usually 45^{o}) to the surface normal as in Figs. A-8 through A-10. The strain

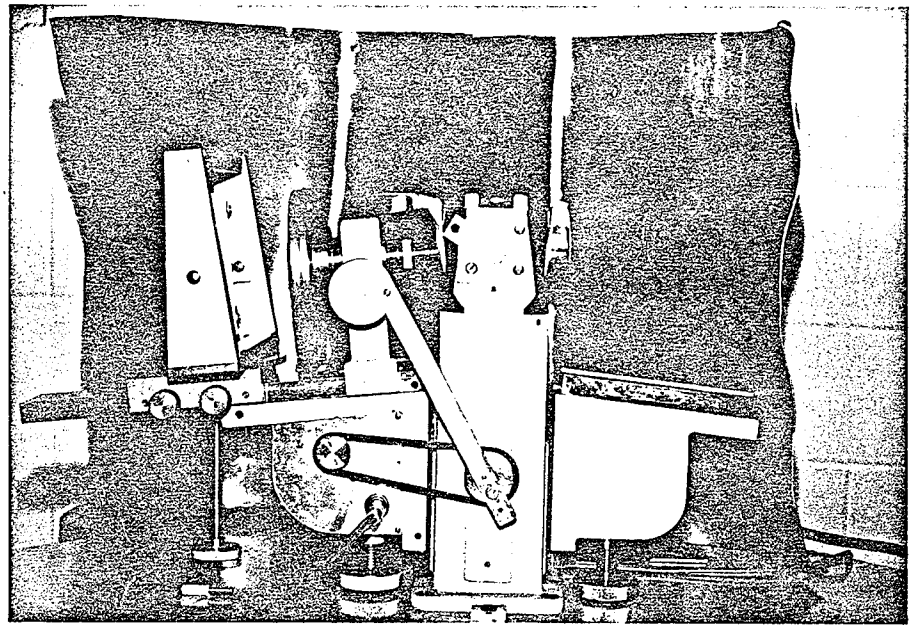

Figure A.6. Normal Incidence Back Reflection Shot

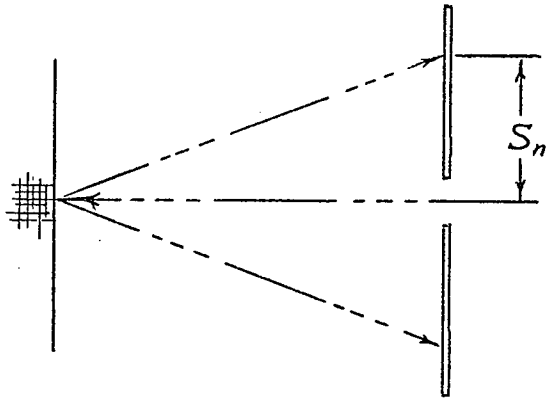

Figure A.7. Normal Incidence Back Reflection Shot

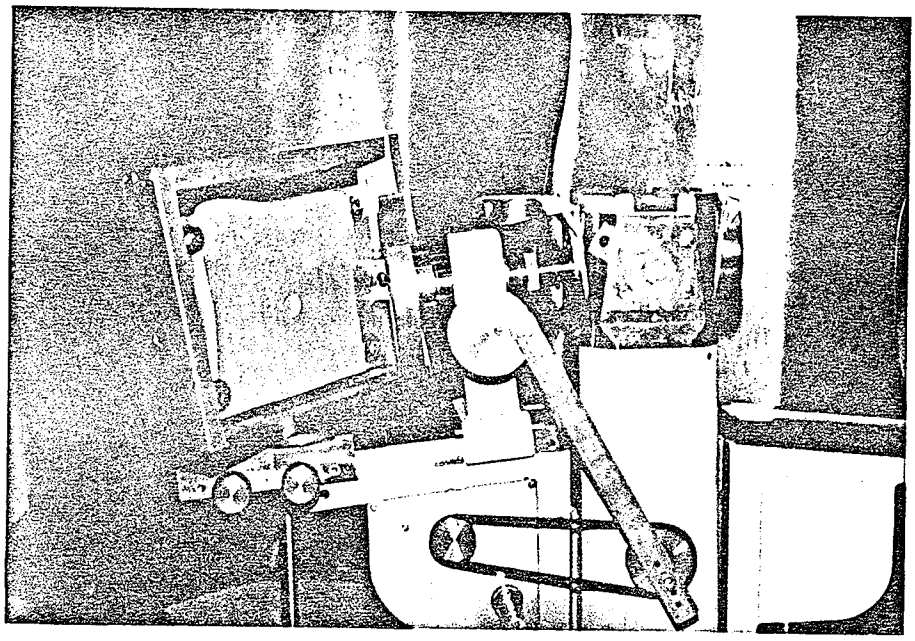

Figure A.8. Inclined Incidence Back Reflection Shot (Radial Stress)

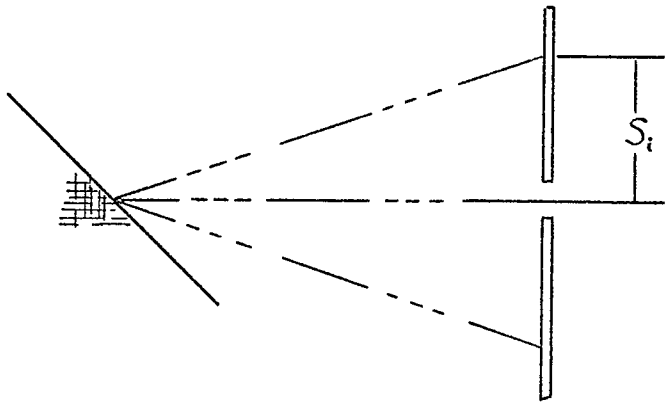

Figure A.9. Inclined Incidence Back Reflection Shot

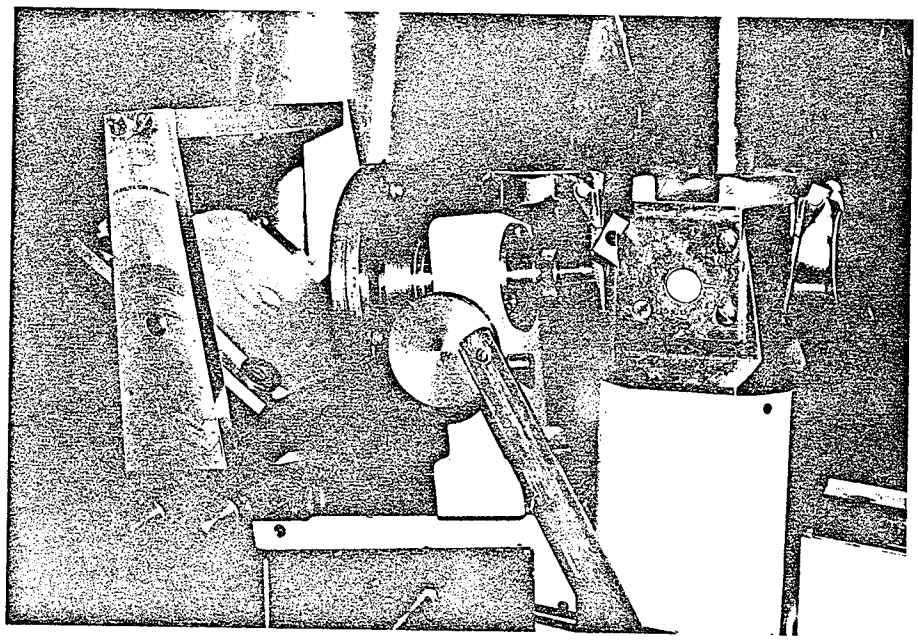

Figure A.10. Inclined Incidence Back Reflection Shot (Tangential Stress)

measured is still in a direction perpendicular to the beam. The inclined strain is:

$$\varepsilon_\psi = \frac{d_\psi - d_o}{d_o}$$

d_ψ = lattice parameter in the 'ϕ' direction, inclined 'ψ^o, strained.

The strain in the normal and 'ϕ' direction may be related through elastic considerations by:

$$\varepsilon_\psi - \varepsilon_n = \frac{\sigma_\phi}{E} (1+\upsilon) \sin^2\psi$$

Here 'σ_ϕ' is the stress in the 'ϕ' direction, 'E' is the material elastic modulus and 'υ' is the Poisson ratio.

The denominator 'd_o' may be replaced by 'd_n' with negligible error and hence:

$$\sigma_\phi = \frac{E}{(1+\upsilon)} \sin^2\psi \quad \frac{(d_\psi - d_n)}{d_n}$$

This equation may be put into a more useful form so that the stress may be computed from the shift in the position of the diffracted ring. First the Bragg Law is differentiated:

$$\frac{d\,(d)}{dt} = \frac{d}{dt} \left(\frac{n\lambda}{2} \frac{1}{\sin\theta}\right)$$

$$\frac{\Delta d}{d} = -\cot\phi \; \Delta\phi$$

The radius of the diffracted ring, 'S' may be related to the distance of the specimen from the film 'D':

$$S = D \tan(180^{o}-2\theta) = - D \tan 2\theta$$

Differentiating

$$\Delta S = - 2D \sec^2 2\theta \, \Delta\theta$$

$$\Delta S = - 2D \sec^2 2\theta \left(-\frac{\Delta d}{d} \tan\theta\right)$$

$$= 2D \sec^2 2\theta \tan\theta \frac{(\Delta d)}{d}$$

and

$$\frac{\Delta d}{d} = \frac{d_\psi - d_n}{d_n} \, , \quad \Delta S = S_i - S_n$$

$$\sigma_\phi = \frac{E}{(1+\upsilon)} \quad \frac{1}{\sin^2\psi} \quad \frac{S_i - S_n}{2D \sec^2 2\theta \tan\theta}$$

The form of the equation is used in computation of stresses in the 'ϕ' direction.

Since there is a hole in the centre of the film the radii of these rings cannot be measured directly. Also, the rings from the inclined incidence shots are not perfectly circular. Fig. A.11 illustrates these rings where planes are symmetrical about the incident beam yet the strain and hence lattice spacing varies

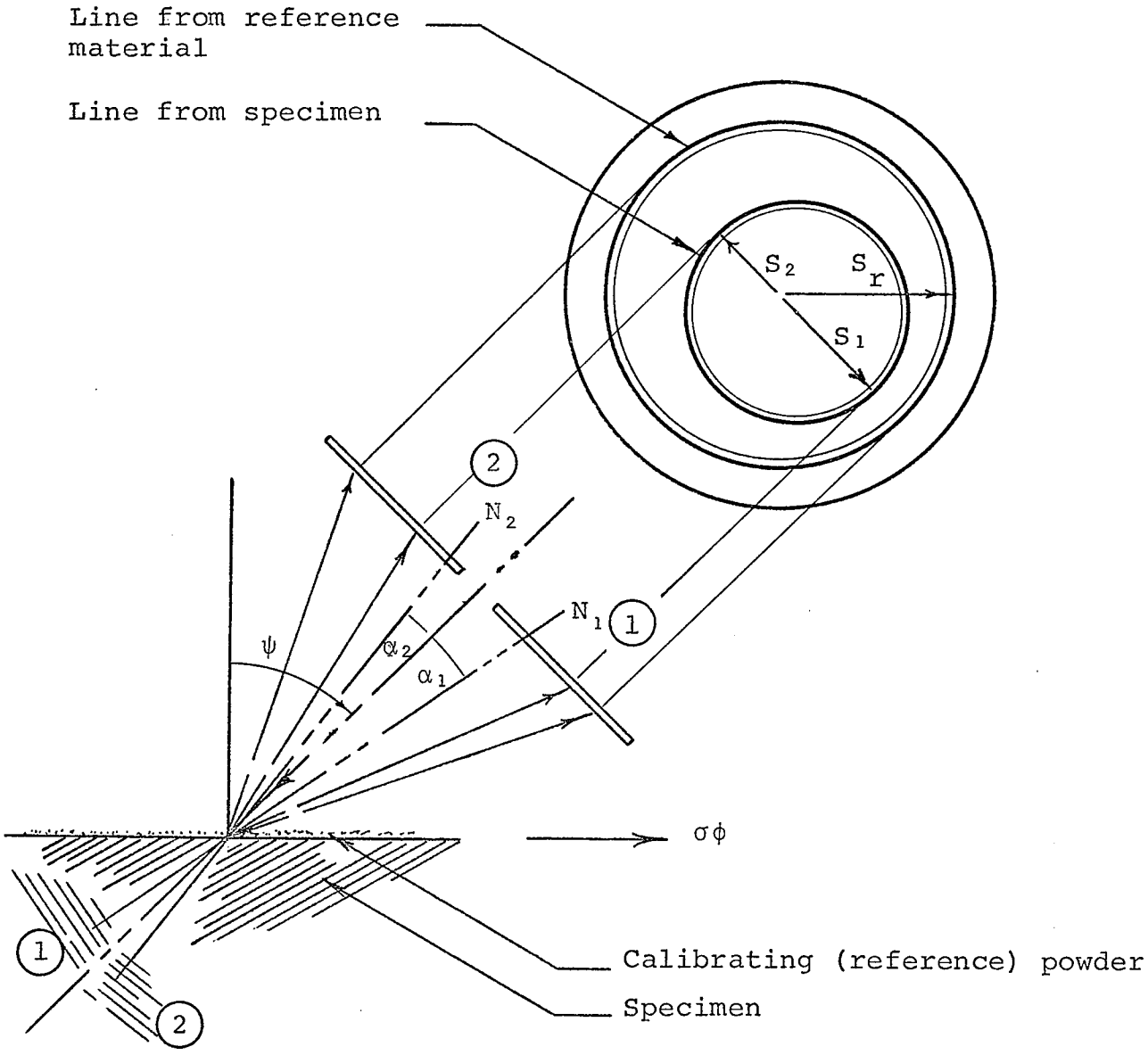

Figure A.11. Eccentricity of Measured Ring at Inclined Incidence due to Unequal Strains in Planes 1 and 2

with the angle between the plane normal and the surface normal. Consequently there are different '2θ' diffraction angles for planes reflecting to the low and high sides of the film. The usual practice is to measure the radial distance at the low side of the film since its position is more sensitive to strain. To measure this distance the center of the film is found using a calibrating powder applied to the specimen surface with a light grease. A calibrating powder is a powder of annealed metal of known lattice parameter which produces a diffraction line in close proximity to the measured line. The center of the film now corresponds to the centre of this reference ring and the desired radial distance on the measured ring may now be found. The reference ring may also serve in accurate calculations of the specimen to film distance.

For the measurements described in this thesis a calibrating strip was used in place of a calibrating powder. This was found necessary because of the low intensity of the aluminum line when a calibrating substance is applied. The reference strip was of pure nickel with a 30 micron grain size. The film was exposed at normal incidence with the nickel in place then double exposed at inclined incidence with the nickel removed.

The accuracy of the x-ray back reflection technique has several limiting factors. Cold working which produces

residual microstrains causes a broadening of the diffraction lines. This makes reading of shifts only approximate. The elastic modulus of the material plays a significant part. The shifts of the diffraction circle will be greater for low modulus materials than for high modulus materials. The choice of diffraction peak also affects the accuracy. The highest precision is obtained when the diffracted ring having the largest 2θ value is used. This is seen from the Bragg law. Since $\sin\theta$ is proportional to $1/d$ for any incident radiation as 'θ' approaches 90^{o}, changes in 'd' produce much greater changes in 'θ'.

In a material with sharp diffraction lines an accuracy of $\pm$ 1200 psi. may be obtained for low modulus aluminums and $\pm$ 3000 psi. for steels. Cold worked materials may commonly be measured to within $\pm$ 2000 to $\pm$ 5000 psi.

A.3 Specimens and Equipment

1. Specimen Preparation

The specimens prepared for fatigue testing were 2024-T3 aluminum, 1 in. x .050 in. with a 5/32 in. pin bore. The stress gradients produced by the dimpling process were suspected to be too high for measurement on these specimens to be practicable. Stress measurements were instead conducted on scaled up models of the

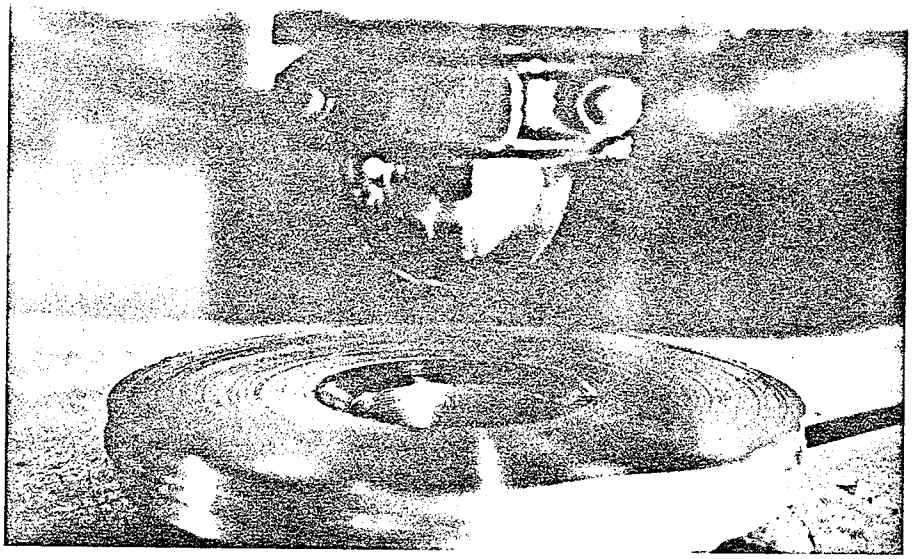

Figure A.12. Scaled Up Indentor and Die

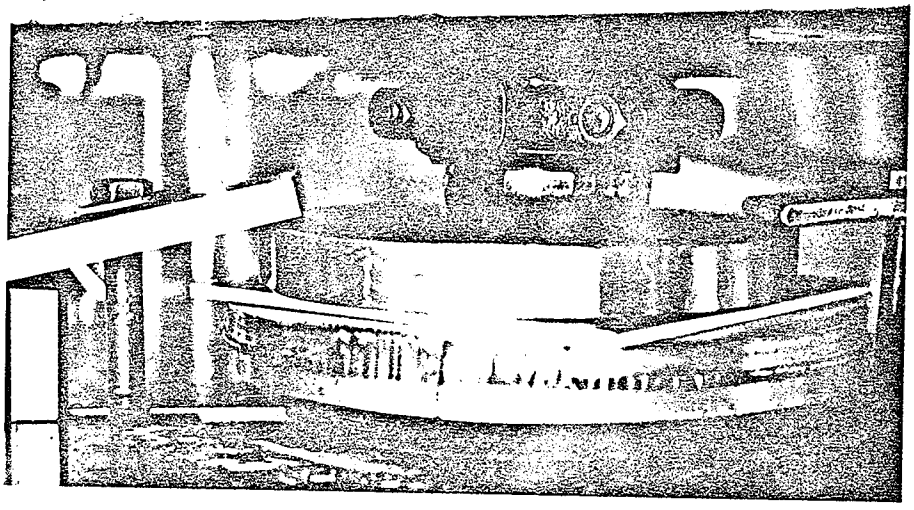

Figure A.13 Dimpling of Scaled Up Specimen for X-Ray Stress Analysis

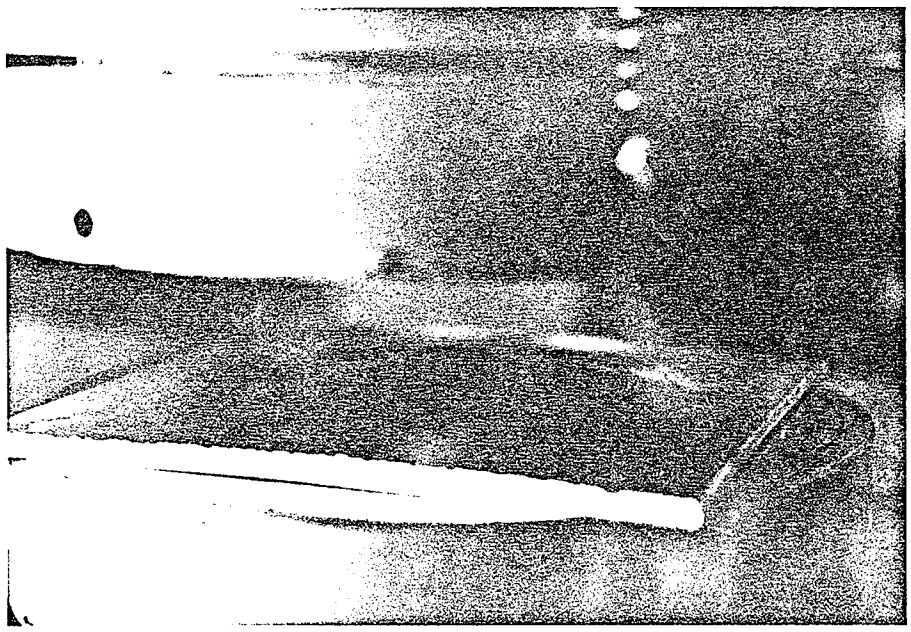

Figure A.14 Flattening of Scaled Up Specimen for X-Ray Stress Analysis

specimen. Dimensional consistency of all specimen and dimpling parameters was maintained with a final specimen of four inches by four inches used. The fatigue specimens were also alclad with pure aluminum. As the x-ray technique measures surface strains only scaled up specimens were of unclad 6061-T6 aluminum which was commercially available. The chemical and physical properties of this alloy are listed in Table A.1.

As indicated, fine grain size is of prime importance in obtaining sharp, easily readable films. To obtain a fine grain size .250 in. 6061-T6 plate was rolled in both directions down to .100 in. thickness then cut to size. This plate was then heat-treated at 410^{o}C for one-half hour to obtain a fine grain structure.

Dimpling of these specimens, illustrated in Fig. A.12 to Fig. A.14, was performed in a large press with correspondingly scaled indentors and dies.

The surface condition of specimens used for x-ray analysis is critical for two reasons. First surface scale and oxides will absorb radiation leaving low intensity patterns requiring unacceptably long exposure times. Secondly any pits, scratches or deep surface asperities will relieve the surface stresses giving erroneous results.

The procedure followed in the surface preparation of x-ray specimens for purposes of this thesis were as follows. First the surface was buffed free of deep scratches

Table A.1

Chemical and Physical Properties

of 6061-T6 Aluminum Alloy

Chemical Properties

Mg	1.0 %
Si	0.6 %
Cu	0.25%
Cr	0.25%

Physical Properties

Ultimate Tensile Strength	45,000 psi.
Yield Strength	40,000 psi.
Fatigue Limit @ 500 x 10^6 cycles	14,000 psi.
Modulus of Elasticity	10.0 x 10^6 psi.

then etched deeply in Tucker's solution. The specimens were next sanded in stages with silcon paper of from 210 to 600 grit. The specimens were then chemically polished at 90°C under agitation in the following solution:

80% ortho-phosphoric acid
12% sulphuric acid
8% nitric acid (36)

The resulting smooth highly reflective surface was suitable for clear, sharp x-ray diffraction patterns.

2. Apparatus

A Philips, Norelco water cooled x-ray diffraction unit was used. The unit is illustrated in Fig. A.15 and conditions of use are described in Table A.2. A camera was designed and built to adapt to the Philips x-ray unit utilizing the powder camera drive to oscillate the film. A Philips 6 cm., 1.0 mm. diameter collimator was positioned to conform to recommendations in the Philips manual on length vs tip to film distances for optimum line sharpness. A biplanar rotating specimen holder was designed and built so that specimens up to 4 ins. x 4 ins. could be rotated about both the horizontal and vertical axes.

The target material used was Cu. A diffractometer pattern for 6061-T6 under Cu-K_α radiation is shown in Fig.A.16. The highest line, at 162°, was used for strain measurement.

A.4 Results of Residual Stress Measurement

Two series of dimpled specimen were measured, Series I and series VIa. Series I was the first series tried and showed

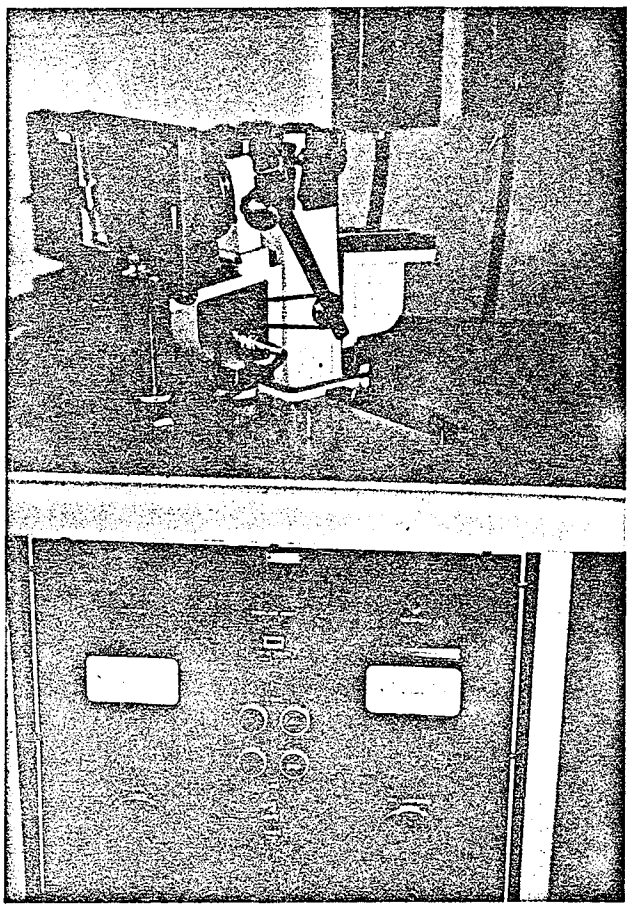

Figure A.15. Philips-Norelco Water Cooled X-Ray Diffraction Unit

Table A.2

Specifications on the Use of the

X-Ray Diffraction Unit

X-ray Unit	Philips-Norelco 12045
Characteristic X-ray	Cu - K_α
Filter	Ni
Diffraction Plane	511/333
Calibration Standard	Ni 30μ grain annealed strip
Specimen to film distance	66 mm.
Power Level	40 kv., 20 ma
Collimation	1.0 mm. diameter double pin-hole
Film Rotation	$\pm$ 12°
Method of Peak Measurement	Visual, Half-value Breadth Method
Exposure time: Calibration	45 min.
Specimen	1 hr. 15 min.
Film	Kodak Medical X-ray Film
Processing	Kodak Medical X-ray Developer and Fixer 7 min. each

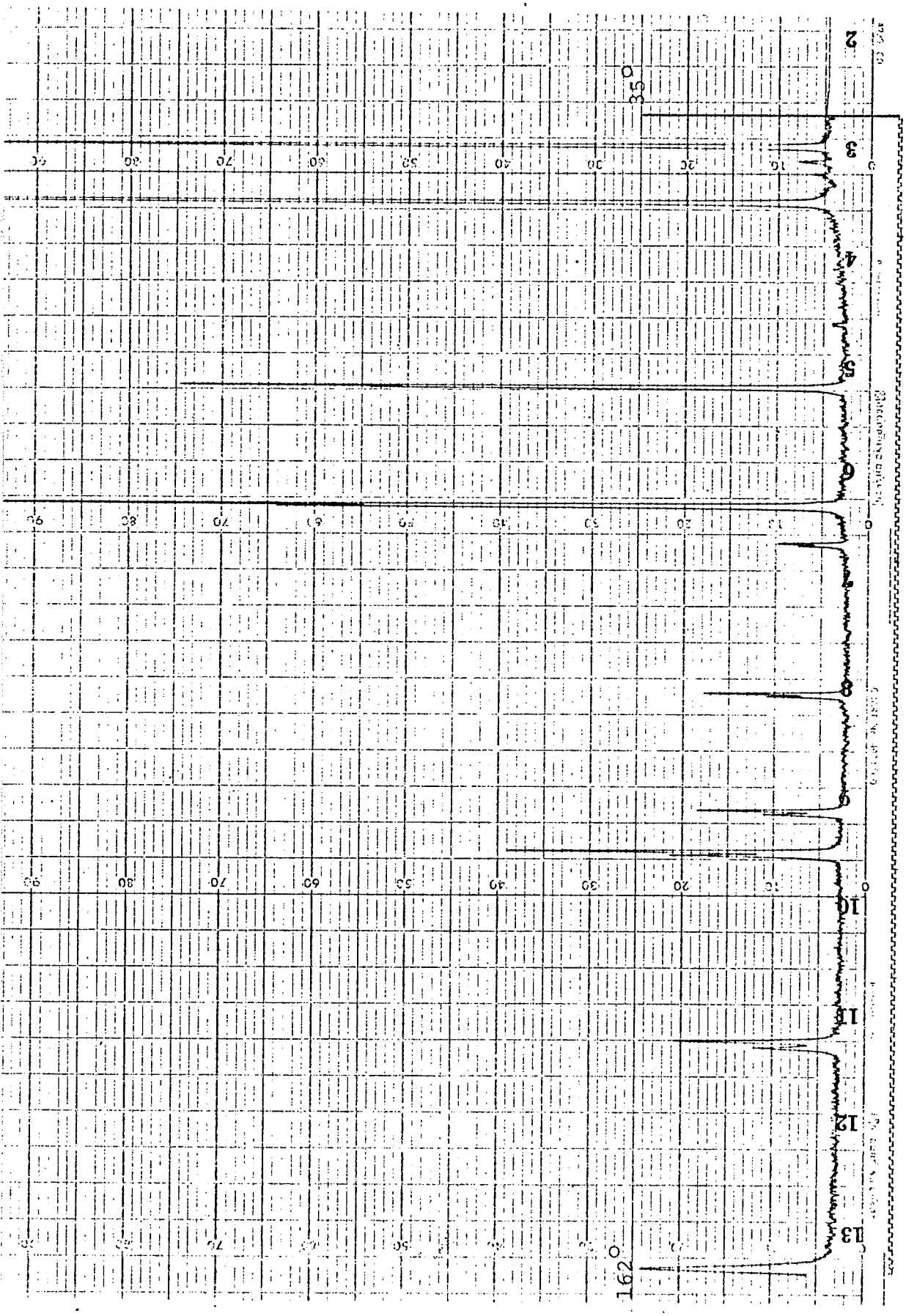

Figure A.16. Diffractometer Pattern of 6061-T6 Aluminum Alloy, Cu - K_α Radiation

intermediate strength improvement. Series VIa showed the greatest fatigue strength improvement in tests described in section four. The stress distributions are repeated from Chapter 3 in Figs. A.17 and A.18 with a sample stress calculation below. The three x-ray exposures at the sample position are shown in Fig. A.19.

Series VIa Dimpling Process

Position: .75 in. from centre on a radial line

Film Data:

Positions of Diffraction Rings Measured by Vernier (cm.)	
Calibration Ring	Aluminum Ring
Film #61 Normal Incidence	24.505 20.385
Film #62 Inclined Incidence 26.890 20.800	Tangential Stress 25.950 21.635
Film #63 Inclined Incidence 27.210 21.180	Radial Stress 26.220 22.010

Aluminum ring normal diameter: 4.120 cm.

Radius (S_n) 2.060 cm.

Calibration Ring diameter 6.060 cm.

Radius 3.030 cm.

Center of Film: Tang. 23.830 cm.

Rad. 24.210 cm.

Specimen to film distance 'D': 6.780 cm.

Lattice parameter for Ni:

2θ: 155.63°

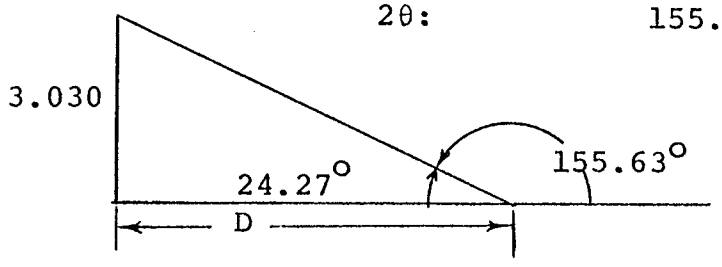

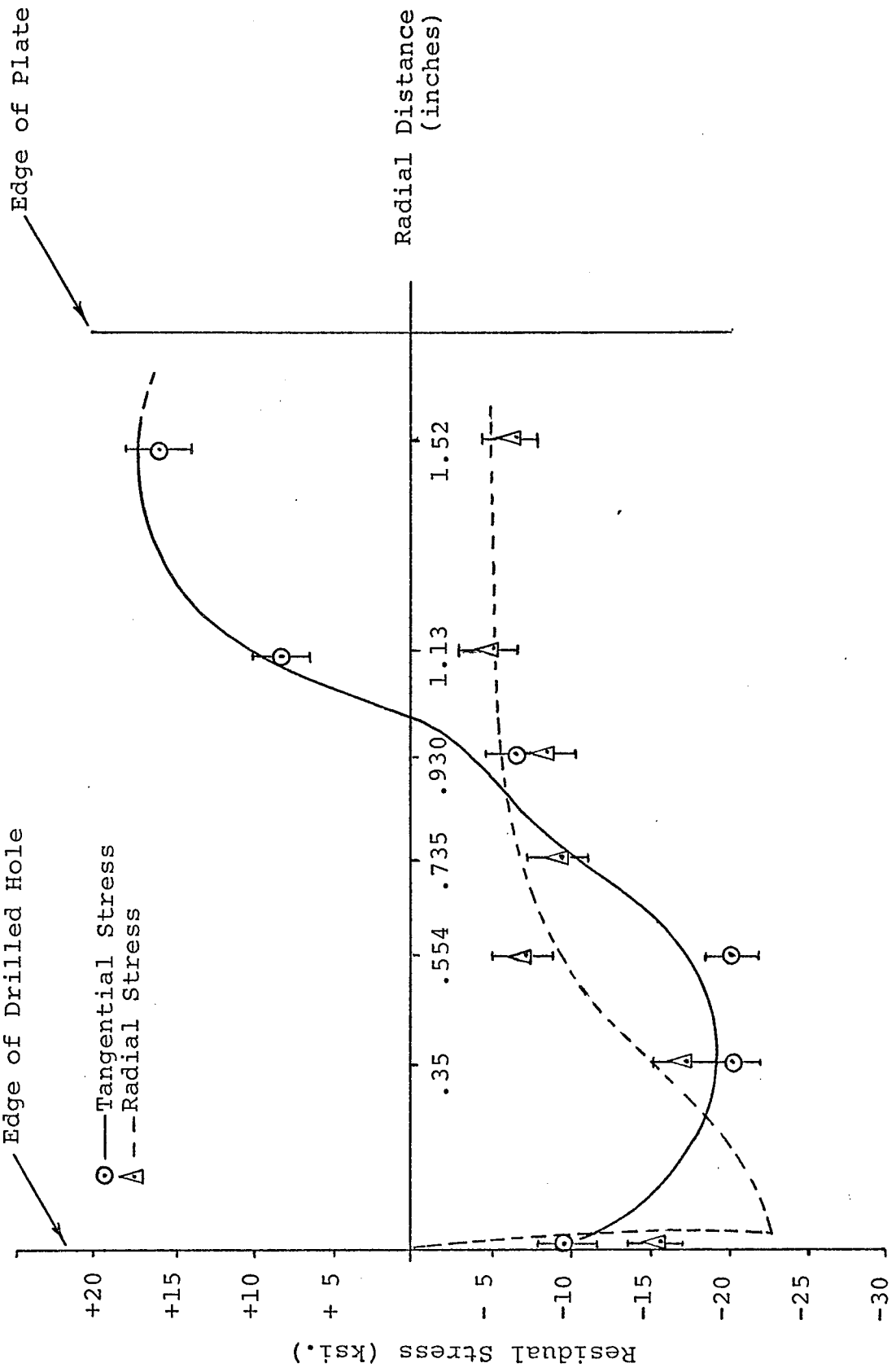

Figure A.17. Residual Stress Distribution on a Series I Dimpled Specimen Determined by X-Ray Diffraction

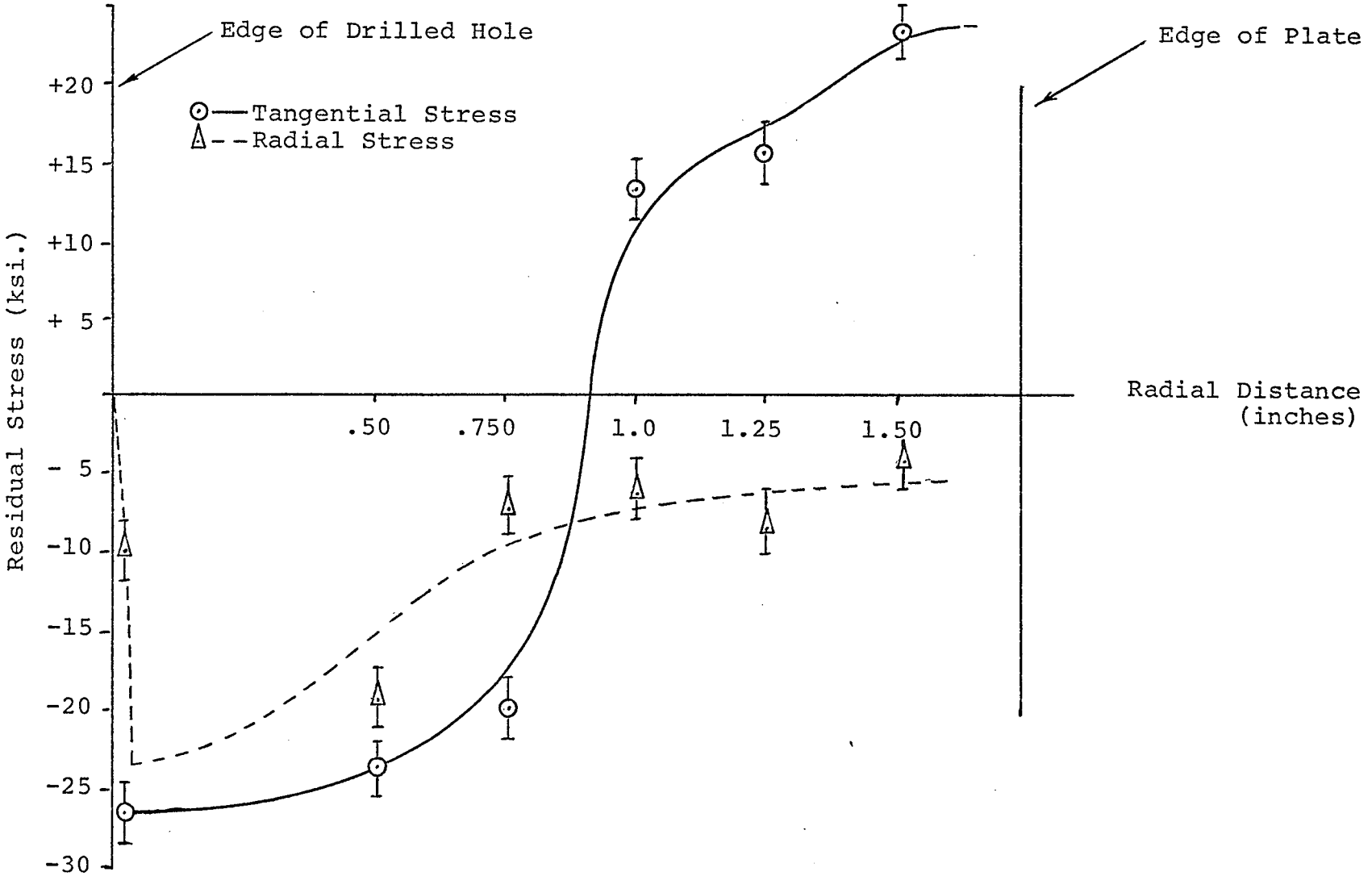

Figure A.18. Residual Stress Distribution in a Series VIa Dimpled Specimen Determined by X-Ray Diffraction

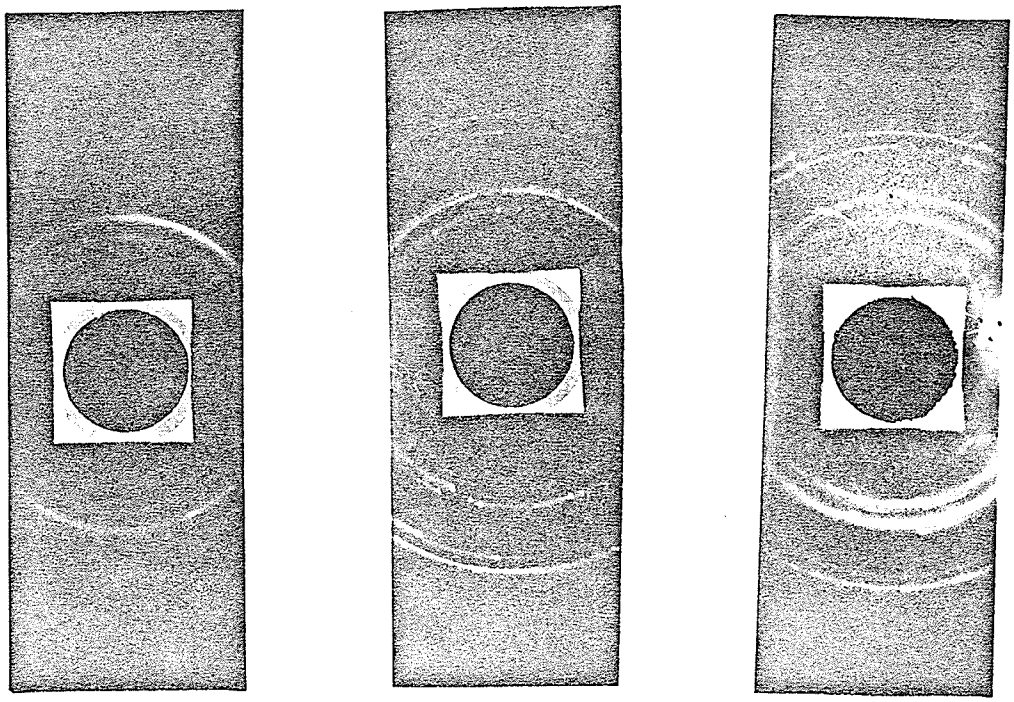

Figure A.19. Back Reflection Exposures a) Normal Incidence, b) Inclined, Tangential Stress, c) Inclined Radial Stress

$\tan (24.27^{\circ}) = .45082$

$$D = \frac{3.030}{.45082} + .05 = 6.730 + .05 = 6.780 \text{ cm.}$$

(Calibration strip thickness .05 cm.)

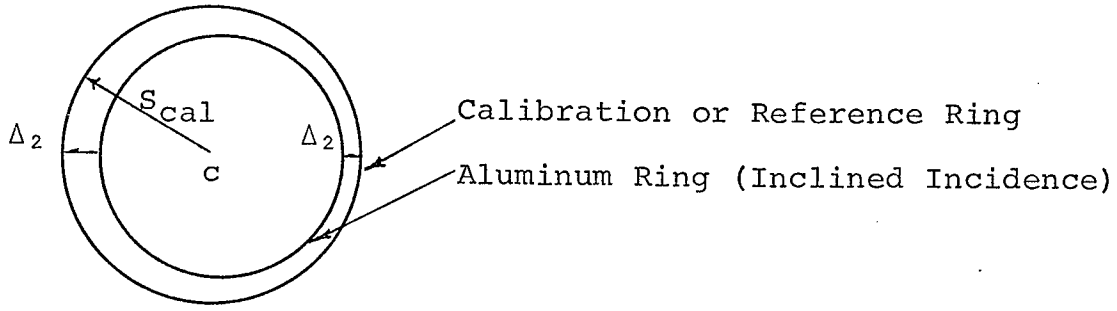

Tangential Stress Calculation

$\Delta_1 = .940$ $\Delta_2 = .835$

$S_2 = S_i = 2.210$ cm.

$S_i - S_n = .150$ cm.

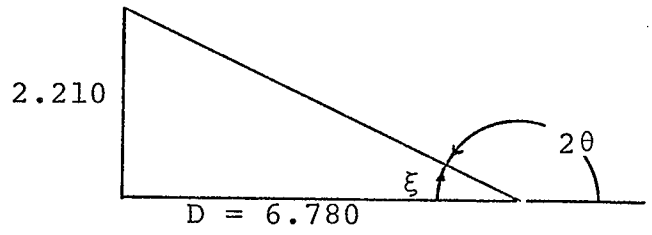

$\tan \xi = \frac{2.210}{6.780} = .331$ $\xi = 18^{\circ}20'$ $2\theta = 161^{\circ}40'$

$\sec 2\theta = 1.0535$ $\sec^2 2\theta = 1.110$ $\tan\theta = 6.1970$

$\sin^2\psi = .500$

$$\underset{\text{Tan.}}{\sigma\phi} = \frac{10 \times 10^6 \quad (.150)}{2\ (6.780) \times 1.33 \times 1.110 \times 6.1970 \times .500}$$

$= 24{,}500$ psi.

Radial Stress Calculation

$\Delta_1 = .990$ $\Delta_2 = .830$

$S_2 = S_i = 2.185$

$S_i - S_n = .125$ cm.

$\tan \xi_r = \frac{2.185}{6.780} = .327$ $\xi_r = 18^\circ 8'$

$2\theta = 161^\circ 52'$

$$\sigma\phi_{Rad.} = \frac{10 \times 10^6 \times .125}{2 \times 6.780 \times 1.33 \times 1.109 \times 6.266 \times .500}$$

$= 20{,}200$ psi.

A check of the x-ray analysis technique was performed on a tension specimen of the same alloy following identical treatment. A strain gauge was placed on the back side of the specimen and from its readings the stress was calculated to be 18,100 psi. The x-ray analysis indicated a stress of 17,500 psi. This value was well within the anticipated range of error of $\pm$ 1800 psi.

A.5 Residual Stress Measurement Using Strain Gauges

As a check on the x-ray diffraction measurements a destructive strain gauge measuring technique was employed on the series VIa specimen.

Both radial and tangential residual strains were measured by placing gauges as in Fig. A.20. In an effort to determine strain variations through the thickness gauges were placed on both sides of the specimen opposite each other. Residual strains were released by removing the strained elements from the surrounding, constraining

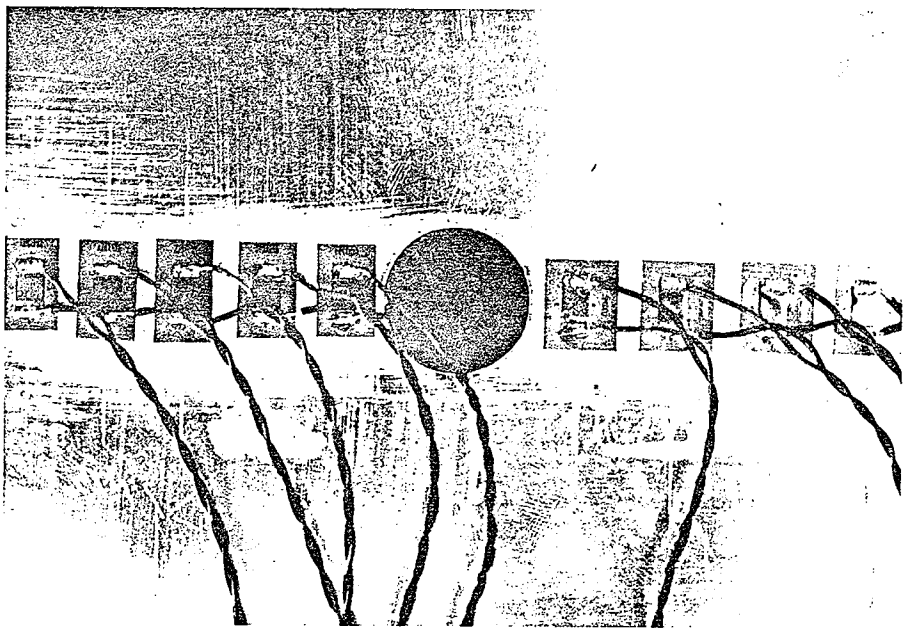

Figure A.20. Strain Gauge Positioning for Destructive Strain Measurements

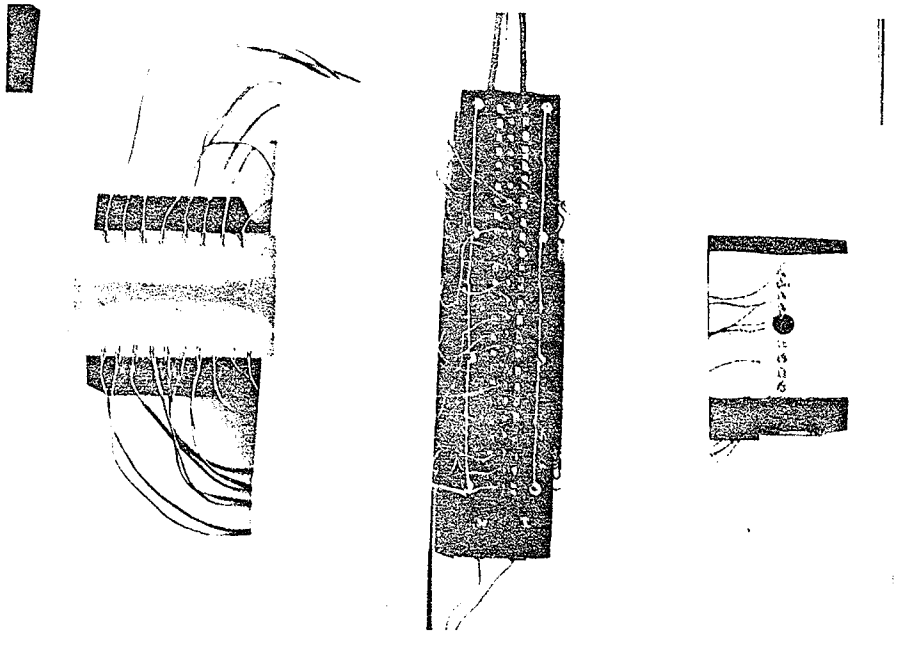

Figure A.21. Remote Bridge Network for Hewlitt-Packard Digital Strain Indicator

material using a fine jewelers' saw. These relaxed strains were measured on a Hewlitt-Packard digital strain indicator. This unit incorporated a remote unbalanced bridge network, shown in Fig. A.21 with each gauge channel comprised of an active gauge, a compensating gauge, and standard resistors to complete a four arm bridge. The voltage and strain readings are presented in Table A.3.

The strain gauge measurements indicated much lower strains than did the x-ray diffraction method. It was conjectured that as a result of scaling up, high strain gradients were set up through the thickness with compression at the edges, tension in the center. This may have prevented complete relief of the residual stresses. The stress levels predicted by the strain gauge measurements were considered insufficient to produce the large differences in fatigue strength observed in the tests described in section four of this thesis.

Table A.3

Voltages and Strains Measured on the Series VIa Dimpled Specimen

Channel	Initial Voltage μV	Final Voltage μV	Strain με
0	8287	6957	424
1	4809	4603	67
2	5335	3985	429
3	4924	4853	22
4	8288	6850	457
5	5594	5491	33
6	9202	8474	232
7	5591	6008	-134
8	691	-2230	-565
9	352	-777	-134
10	-13264	79037	-1650
11	5344	3839	480
12	2013	2424	-132
13	479	261	69
14	-17581	-16372	-388
15	6152	7314	-370
16	4588	6464	-600
17	5266	6871	-513
18 Battery	3.0174 Volts	3.0153 Volts	

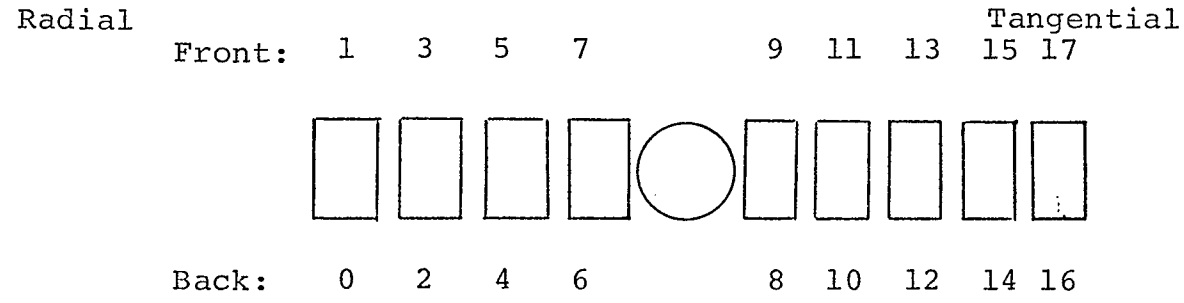

Appendix B

Comparative Brittle Lacquer Stress Determination

Comparative tension tests were performed on two similar aluminum fatigue specimens, one drilled and one dimpled and drilled. Both were coated with brittle strain indicating lacquer which flakes off as the yield stress is reached. Knowing the tensile load at yield for each specimen the residual stress at the hole edge may be determined as follows:

Load Levels:

F(drilled) = 1200 lb.

F(dimpled) = 1700 lb.

Nominal Stress Levels:

σ(drilled) = 1200/((1.5 - .125) x .050)

= 17,400 psi.

σ(dimpled) = 1700/.068 = 24,800 psi.

Stress Concentration Factor:

K_t = 2.65 *Faires (82)

Peak Stress at the Hole Edge:

σ_p(drilled) = 17,400 x 2.65 = 46,400 psi.

σ_p(dimpled) = 24,800 x 2.65 = 65,600 psi.

Residual Stress = (σ_p(dimpled) - σ_p(drilled))

= 19,200 psi.